1,2-Asymmetric Induction in Carbonyl Compounds - A Computational Study

by

Jeffrey Retallick

B.Sc., University of New Brunswick, 2015

A THESIS SUBMITTED IN PARTIAL FULFILLMENT OF THE REQUIREMENTS FOR THE DEGREE OF

Master of Science

In the Graduate Academic Unit of Chemistry

Supervisor(s):	Ghislain Deslongchamps, Ph.D., Chemistry
Examining Board:	Rodney Cooper, M.Sc., Computer Science, Chair
External Examiner:	Ben Newling, Ph.D., Physics

This thesis is accepted by the
Dean of Graduate Studies

THE UNIVERSITY OF NEW BRUNSWICK

October, 2019

Abstract

In asymmetric synthesis, it is important to reliably predict the major stereoisomeric product of a reaction. One such reaction is the nucleophilic addition to a carbonyl compound featuring an adjacent chiral carbon. Several reaction models exist in literature to predict the facial selectivity of these reactions. These models provide simple visual drawings to quickly predict the major product of such a reaction without requiring exhaustive quantum mechanical calculations. These models are used on a daily basis, and some models perform better than others, making it valuable to investigate which ones are the most effective.

For the first time in this thesis, high-level computations have been performed on all of the literature models to verify their efficacy. The results of this thesis offers a definitive answer that the Felkin-Anh and Wintner models are the most effective, and that bent bond theory offers an interesting insight on the mechanics of these reactions.

Dedication

Kyle, Nan, and Taryn.

Acknowledgements

Thanks to my family for their support.

Ghislain, thank you for putting up with me over the past while. I learned some valuable lessons about life, chemistry, and extreme programming. Encountering difficulties during graduate studies is not something that is unique to me, but thank you for offering your unending patience as I went through this process.

Rod, thank you for always offering your council when I needed it. You helped me see things from another perspective and kept me grounded when I was drifting. Thanks for reminding me about Wolf Wednesday so that I didn't miss it.

Val, thank you for your support and for not hesitating to be on my committee even though you have more than enough responsibilities.

Thank you to Andreas Lambropoulos for your expert services whenever there was an issue with SVL.

Thank you to Dr. Tait for your conversations, your advice, and the lovely green mug.

Table of Contents

List of Tables

List of Figures

List of Symbols and Abbreviations

Abbreviations:

BBAH = Bent Bond Antiperiplanar Hypothesis

FA = Felkin-Anh

GI_MOE = Gaussian Interface for MOE

GS = Ground state

MC = Modified Cornforth

MM = Molecular mechanics

MOE = Molecular Operating Environment

PES = Potential energy scan

PFA = Polar Felkin-Anh

QM = Quantum mechanics

TS = Transition state

Symbols:

alpha: α, denotes the carbon adjacent to the carbonyl carbon

double dagger: ‡, denotes a transition state

pi: π, a bonding pattern

sigma: σ, a bonding pattern

tau: τ, a bonding pattern

Chapter 1

Introduction

An important pursuit of many organic chemists is to find new ways to form C-C bonds. The purpose of this thesis is to look at one of these types of reactions. The reaction in question is the asymmetric addition of a nucleophile to α-chiral aldehydes, and the particular focus of the thesis are the methods that are employed to predict the outcome of these types of reactions. The goal is to expand upon what is known about the topic and to present some quantitative evidence to help determine which of the existing predictive models are the most reliable. To fully understand the problem, it is important to look at what was known in the early to mid 1900s and follow the endeavours of many scientists from then until now.

Carbonyl addition chemistry was known and was being performed in the early 20th century. It was possible to take a carbonyl compound, the simplest being an aldehyde, and add a nucleophile to the electrophilic carbon. For non-chiral carbonyl compounds, the two faces of the carbonyl are enantiotopic: the reaction produces a 50/50 (racemic) mixture of two enantiomeric products, as there is nothing in the system to cause a preference for addition to one face of the carbonyl over the other (Figure 1.1).

However, when the reaction is performed on a carbonyl compound bearing one or more stereogenic centers, the product ratio is never 1:1. Instead, a major product and a minor product are obtained (Figure 1.2) as the two faces of the carbonyl compound are now diastereotopic, meaning that its chirality causes a preference for the addition to occur on one face of the carbonyl over the other.

Many questions arise from these experimental observations: What interactions cause this bias in the product distributions? How could the major product be predicted? Could the reaction be controlled in such a way that only one of the diastereomeric products is obtained?

When the carbonyl compound has a stereogenic center adjacent to the carbonyl group, the influence of that chiral center on the nucleophilic addition is referred to as *1,2-asymmetric induction*. In other words, one stereogenic center induces the chirality of a new stereogenic center at the adjacent position upon nucleophilic addition.

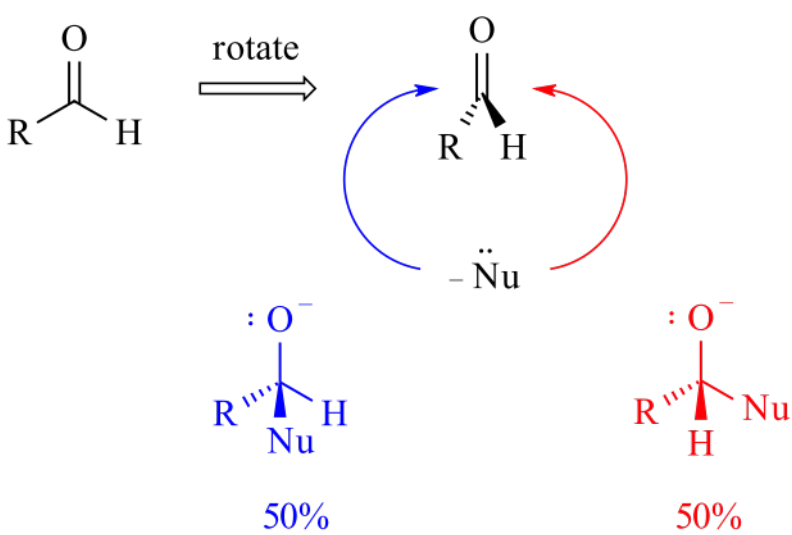

Figure 1.1: A nucleophile can add to the two enantiotopic faces of an aldehyde, one depicted in red and the other in blue. The result is two enantiomers each in a 1:1 ratio. Nu = Nucleophile, R = alkyl group.

Understanding and controlling the outcome of asymmetric reactions allows for more efficient syntheses of chiral natural products or enantiopure drugs, and paves the way for novel reactions. It is for these reasons that many scientists set out to discover what exactly was going on. The next chapter outlines the more influential contributors to this area and their work.

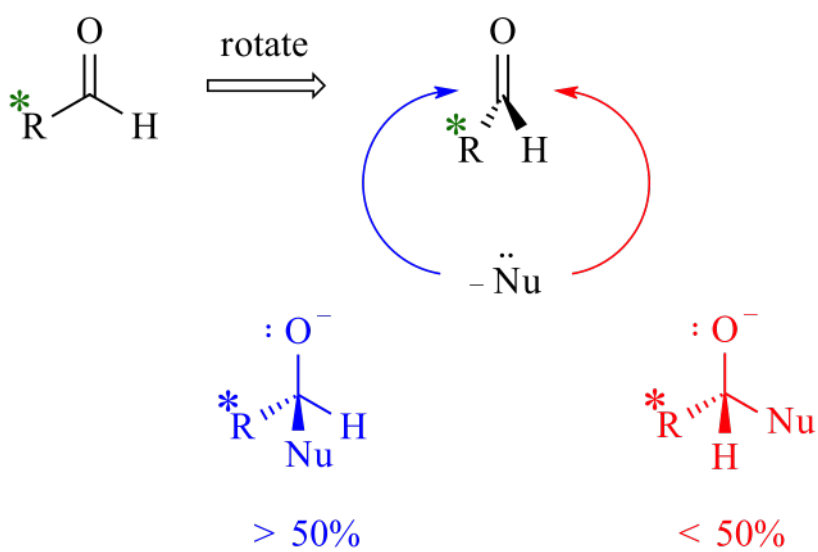

Figure 1.2: A nucleophile can add to the two diastereotopic faces of a chiral aldehyde. The two different additions are shown in red and blue. The result is one diastereomer in higher yield than the other (*R = chiral group)

Chapter 2

A history of influential asymmetric models in the literature

2.1 Non-polar models for asymmetric induction

The following section summarizes the most influential models in the literature to account for the 1-2 asymmetric induction on carbonyl compounds where the three substituents on the stereogenic α-carbon are non-polar, predominantly alkyl groups.

2.1.1 Cram model (1952)

2.1.1.1 Deriving a predictive model of diastereoselectivity

The first group to develop a model to try and explain this trend of diastereoselectivity in optically active carbonyls was D. J. Cram and F. A. A. Elhafez.[1] They looked at a series of experiments in which optically active α-chiral ketones were reacted with either hydride or alkyl nucleophiles to yield 2° and 3° alcohols, respectively as shown in Figure 2.1. In each case, the asymmetry in the reactant molecule induced a bias in the reduction reaction to form one alcohol diastereomer preferentially over the other.

Table 2.1: Relative abundance of *erythro* and *threo* isomers isolated from various Grignard reactions and lithium aluminum hydride reactions, see Figure 2.1. Data reproduced from Cram 1952.[1] R" = C_6H_5.

R'	R	Reagent	Prediction	*erythro*	*threo*
CH_3	H	CH_3MgI	*erythro*	2	1
C_2H_5	H	CH_3MgI	*erythro*	2.5	1
CH_3	H	C_2H_5MgBr	*erythro*	3	1
CH_3	C_6H_5	$LiAlH_4$	*erythro*	>4	1
CH_3	CH_3	$LiAlH_4$	*threo*	1	2.5
C_2H_5	CH_3	$LiAlH_4$	*threo*	1	3
CH_3	C_2H_5	$LiAlH_4$	*threo*	1	2
CH_3	H	C_6H_5MgBr	*threo*	1	>4

For each of these reactions, the major configuration of the newly formed chiral center could be inverted by inverting the configuration of the α-carbon stereocenter of the ketone. Cram and Elhafez proposed that the major product in these reactions could be predicted on steric grounds. They then investigated and presented eight reactions to support their observations. Grignard (RMgX) reactions and lithium aluminum hydride ($LiAlH_4$) reductions were performed. Their results can be seen in Table 2.1. *Threo* and *erythro* are old terms that refer to different configurations of diastereomers (Figure 2.2).

Based on these results, a model was proposed for predicting the major diastereomer for re-

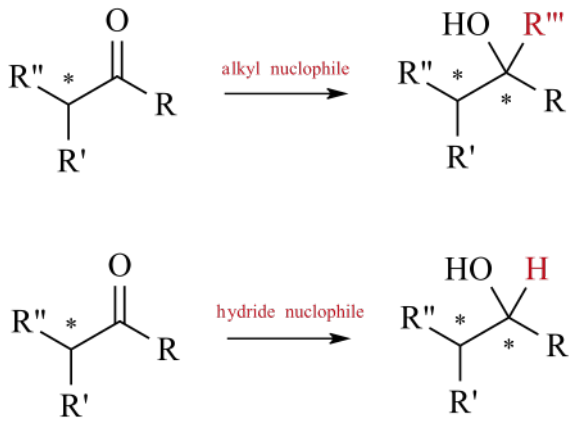

Figure 2.1: Reacting asymmetric ketones with alkyl and hydride nucleophiles.

actions with asymmetric carbonyl compounds. The model was called "The Rule of Steric Control of Asymmetric Induction" and is referred to today as Cram's Rule (Figure 2.3).

2.1.1.2 How Models Will Be Compared

Before the rationale behind Cram's rule is outlined, it is important to understand the different elements of a predictive model. This is the first of many models that will be explored in this thesis, and they will all be approached in a similar manner. The two most important aspects to consider for each model are 1) the conformation of the α-chiral substrate, i.e. the positions of the α-carbon substituents relative to the carbonyl group based on rotation

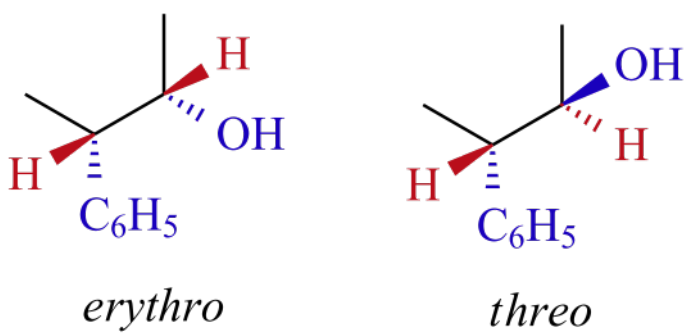

Figure 2.2: In the *erythro* configuration, at least two highly similar sets of substituents (in this case, methyl and H) eclipse each other in one of the three eclipsed conformations. *Threo* refers to the other diastereomer, where the three substituents never eclipse each other in this way.

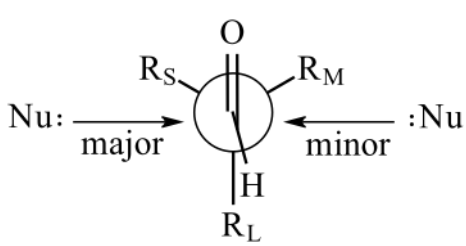

Figure 2.3: Cram's rule: R groups labeled in order of increasing steric bulk, $R_S < R_M < R_L$. The arrows denote whether addition to that diastereotopic face of the carbonyl will lead to the major or minor product. Approach of the nucleophile from the least hindered side is expected to yield the major product.

of the α-carbon–carbonyl carbon bond and 2) the trajectory of the incoming nucleophile. These two characteristics are what set up the geometry of the carbonyl-nucleophile system. Correctly positioning all atoms in space at the bond-breaking-and-forming step is crucial to properly investigate what kinds of interactions are happening as bonds are being broken and formed at the transition state (TS). Being able to correctly identify what types of stabilizing and destabilizing interactions that occur at this step, and correctly estimating the weight of these different interactions (steric, electronic, etc.) is what facilitates the ability to predict facial selectivity. This is what makes a good model.

2.1.1.3 The Rationale Behind Cram's Rule

Cram's rule assumes that the α-chiral carbonyl compound reacts in its more stable ground-state conformation. It argues that the carbonyl oxygen should be considered the largest group, especially since it can coordinate with the metal-containing reagents used in the reaction. This oxygen would then stagger itself between the small and medium alkyl groups of the α-carbon stereocenter, leaving the large group anti to the carbonyl oxygen. The nucleophile would then approach from the least hindered face of the carbonyl group, at an angle perpendicular to the π bond of the carbonyl in order to maximize overlap between the occupied orbital of the incoming nucleophile and the antibonding orbital of the C=O group (π*). According to the Cram model, if the α-carbon stereocenter has the (S) absolute configuration, the nucleophilic addition will occur preferentially from its si face. The reason for this is that the carbonyl oxygen encounters less steric bulk when R_L is placed anti to the carbonyl. When R_M is oriented anti to the carbonyl group, the oxygen is flanked by the R_L group which is less stable. This model is based on reactant ground states without consideration of the reaction transition states, a factor which will be discussed later. Nevertheless, the Cram model is still taught in organic chemistry textbooks today due to its simplicity.

2.1.1.4 Cram Chelate Model

There are situations where Cram's model does not predict the correct product and required elaboration on Cram's part. One case is where one of the substituents on the α-carbon can coordinate to the metal of the reagent, such as an alcohol or an amine on the α-carbon. This would result in chelation of the metal of the reagent between the carbonyl oxygen and one of the α-substituents thereby orienting the carbonyl compound in a way where the two groups eclipse each other, preventing the molecule to adopt the conformation proposed in the Cram model. Cram proposed an additional model to explain this recurring case, called the Cram-chelate model (Figure 2.4), to predict the outcome of such reactions, as they consistently yield the opposite product (i.e. the anti-Cram product) from what would be predicted by Cram's rule.[2] The nucleophile is still assumed to attack perpendicularly to the carbonyl group, but adds from the opposite face, encountering the smaller α-carbon substituent. Few argue about the validity of the Cram chelate model as the molecule is locked in this geometry by fairly strong chelation forces. Cram's rule, however, is a different story as we will see in the next section.

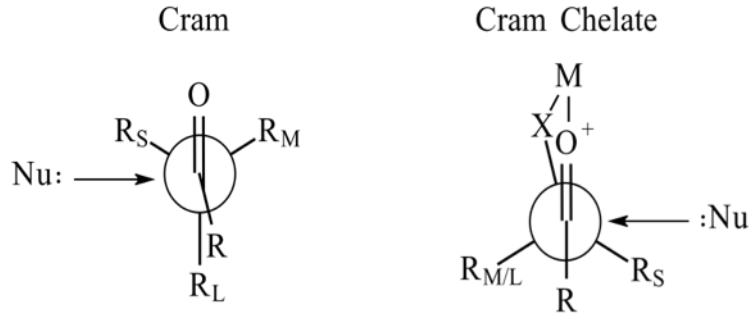

Figure 2.4: Cram's rule compared to the Cram chelate rule. The major product for the Cram chelate case is the anti-Cram product, as the nucleophile adds to the other face of the carbonyl.

2.1.2 Karabatsos model (1967)

The next group to model the stereoselective carbonyl addition was Gerasimos J. Karabatsos.[3] In his paper he discusses some features of Cram's rule that did not seem coherent with the conventional understanding of chemical reactivity.

A case where the diastereomeric ratio of the products decreases with increasing bulk of the R group demonstrates that Cram's rule may not be an accurate depiction of the transition state (Figure 2.5). One would think that as the face that yields product B becomes more sterically hindered, the nucleophile would favor approaching the opposing face yielding A, and increase the A/B product ratio. However, as the size of R increased from Me $<$ Et $<$ *i*-Pr, Karabatsos instead observed a decrease in the A/B product ratio.

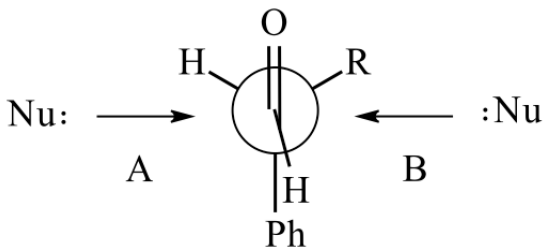

R	A/B
Me	2-4/1
Et	2.5/1
i-Pr	1, 1.3, 1.9/1

Figure 2.5: The diastereomeric ratio varies with different sized R groups on the α-carbon, but in the opposite direction predicted by Cram's rule. Based on Figure IV of Kerabatsos' paper.[3]

Karabatsos challenges the idea that the oxygen is effectively the bulkiest group (as proposed by Cram); based on some new evidence, he proposes that in the more stable form of the reactant, the carbonyl eclipses one of the substituents of the α-carbon.[4] This can be easily visualized using the bent bond model even though this was not used by Karabatsos in this study (Figure 2.6). Indeed, the more stable conformation of carbonyl compounds appears to be eclipsed when represented as Hückel (σ/π) double bonds, whereas it is naturally staggered when represented as Slater/Pauling bent bonds (tau-bonds, τ-bonds).[5–7]

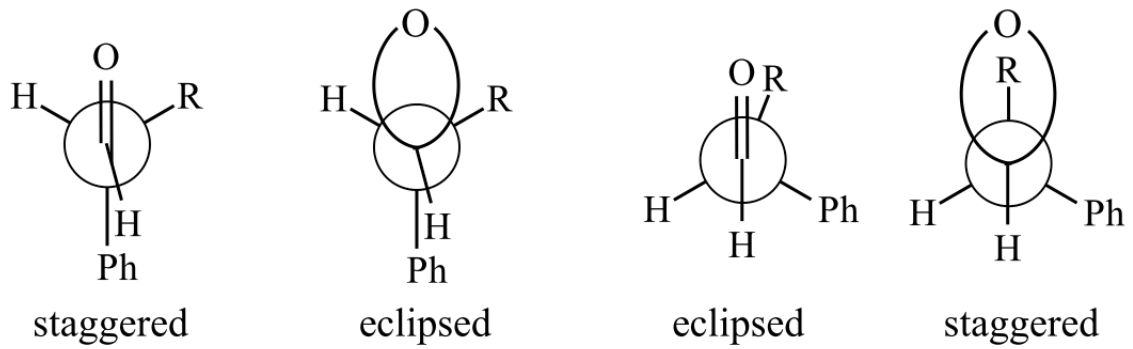

Figure 2.6: A representation of how unsaturated systems can appear eclipsed or staggered depending on how multiple bonding is represented.

The bulkiness of the oxygen and the necessity for it to be placed anti to the large substituent was one of the key features of Cram's rule. If this is not representative of the most stable transition state, it is possible that the success of Cram's rule may not be due to Cram's rule demonstrating the proper reactive conformation of the α-chiral aldehyde. Cram's rule may be the result of fitting empirical results to a model that successfully predicted the outcome of many reactions by coincidence. Clearly a new approach could shed more light on to what is happening in this reaction.

Karabatsos describes his model as follows: He argues that the rotation of the single bond between the carbonyl and α-carbon is low in energy compared to the energy involved in Grignard reactions and hydride reductions. According to the Curtin-Hammett principle (see Appendix A.1), the diastereomeric ratio will then depend only on the difference in the activation energies of the two transition states that lead to each of the diastereomeric products. This would require some knowledge of the two relevant transition state geometries in order to predict the ratio of diastereomeric products.

Karabatsos also uses Hammond's postulate (see Appendix A.2) to describe what the ge-

ometry of the transition states will look like and get a clearer picture on what interactions will predominate. Due to the reactive, exothermic nature of these reactions, it is assumed that the transition state for their rate-determining step, i.e. the addition of the nucleophiles to the carbonyl group, will be reactant-like. A reactant-like transition state will be assumed to have little bond breaking and forming, causing the geometry of the transition state to more closely resemble the reactants than the products. This means that one of the substituents of the α-carbon could eclipse the carbonyl group, and influence the facial selectivity of the reaction.

Karabatsos assumes, like Cram, that the trajectory of the nucleophile will be perpendicular to the carbonyl group (as discussed before, to maximize overlap between the $\pi^*_{C=O}$ orbital and the orbital that describes the lone pair of the incoming nucleophile). With these qualitative considerations in mind, Karabatsos presents six geometries (Figure 2.7) for addition to the two diastereotopic faces that have potential to be the lowest energy transition state, three for each diastereomer (I, I', I" and II, II', II").

Karabatsos argues the relative importance of interactions that contribute to the overall stability of the transition states are firstly the interactions involved in the nucleophilic trajectory and then steric interactions encountered by O and R. If he is correct, then the interactions that disrupt the trajectory of the nucleophile are the most important. If we inspect the interactions between the carbonyl compound and the incoming nucleophile in Figure 2.7, it is clear that geometries I and II are the most favourable, as the nucleophile approaches near the smallest group in these two cases. These two structures account for the product ratio and illustrate Karabatsos's model, Figure 2.8.

Karabatsos' model brought the scientific community one step closer to solving the problem by drawing attention to how steric strain caused by rotational energy barriers in the

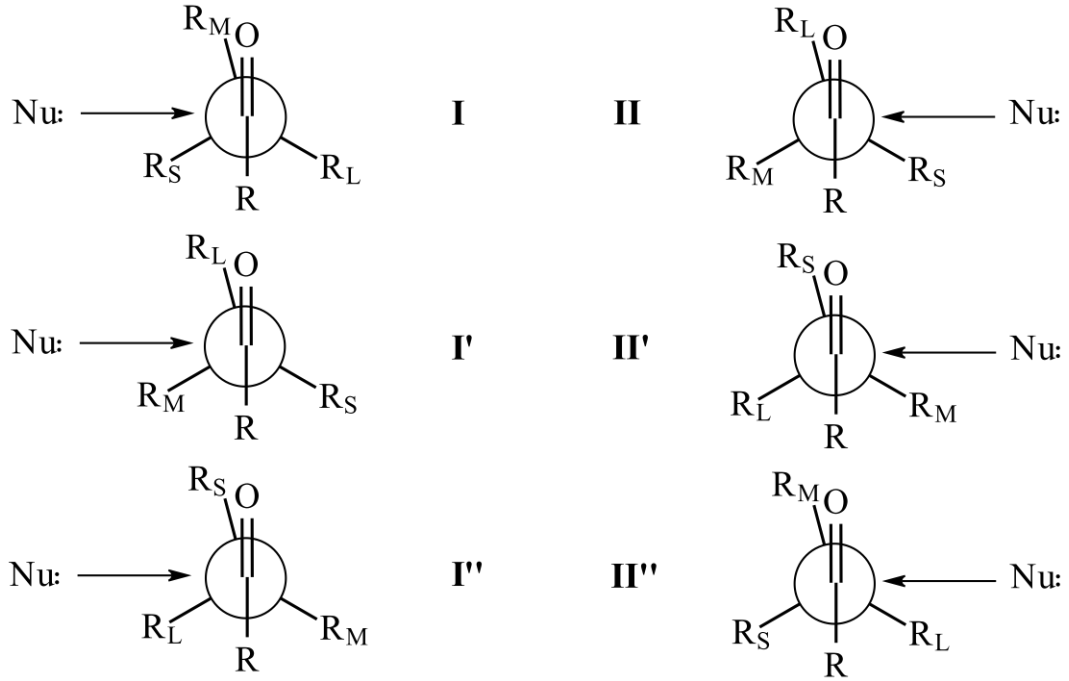

Figure 2.7: Transition state geometries proposed by Karabatsos to have the lowest energies.

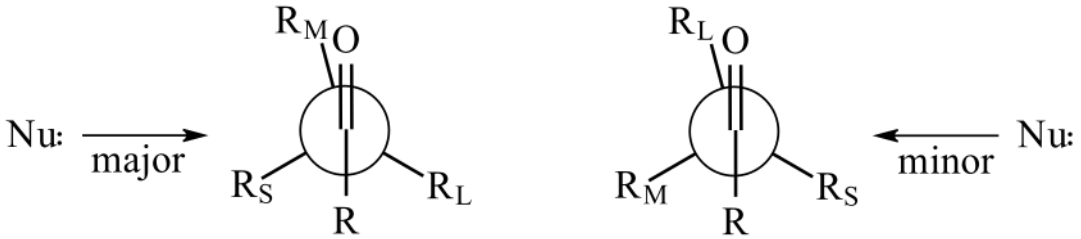

Figure 2.8: The Karabatsos model. R groups labeled in order of increasing steric bulk, $R_S < R_M < R_L$.

ground state are negligible compared to the activation energy. This model also contributes by discussing the importance of prioritizing nucleophilic trajectory and an unhindered path for the nucleophile. However, the story does not end here. Other groups continue to optimize the geometry of this reaction.

2.1.3 Felkin model (1968)

Marc Chérest, Hugh Felkin, and Nicole Prudent describe why Cram and Karabatsos have holes in their approaches and offer an improvement.[8] Here are two reasons why they are unsatisfied with Cram and Karabastos' takes on the situation:

2.1.3.1 Cram/Karabatsos Models Criticism #1

Felkin *et al.* were not convinced that reduction of acyclic ketones should differ significantly from cyclic ketones. As shown in Figure 2.9, applying the Cram and Karabatsos models to cyclohexanones predict hydride addition from the least hindered side of the carbonyl. This would yield *cis* 2-methyl-cyclohexanol as the major product. However, the major product was experimentally determined to be *trans* 2-methyl-cyclohexanol, so something is clearly wrong with the transition state proposed by Karabatsos, and even more so with Cram.[9,10]

2.1.3.2 Cram/Karabatsos Models Criticism #2

In both Cram and Karabatsos' models, the major product geometry places the R group closer to the R_L group when compared to the transition state that yields the minor product. Thus the reaction diastereoselectivity should decrease with increasing size of R, as the steric clash between R and R_L would increase, causing the transition state geometry to

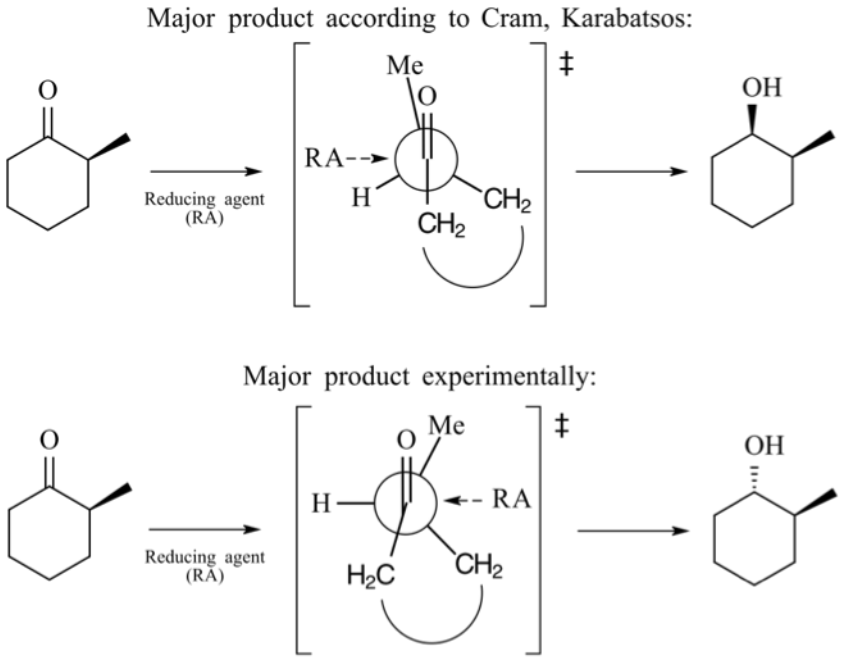

Figure 2.9: Reacting 2-methyl-cyclohexanone with a reducing agent (RA) to test the predictive capabilities of Cram and Karabatsos' models on simple cyclic systems. Upon reduction of the ketone, the models predict the major product to be *cis* 2-methyl-cyclohexanol, while the major product was found to be the *trans* isomer. Semi-circle line drawn to symbolize cyclohexane ring.

become less favorable. It can be seen in Figure 2.10 that a bulky group (R = *t*-Bu) on the ketone is far more selective than an Et or Me group in the same R position.

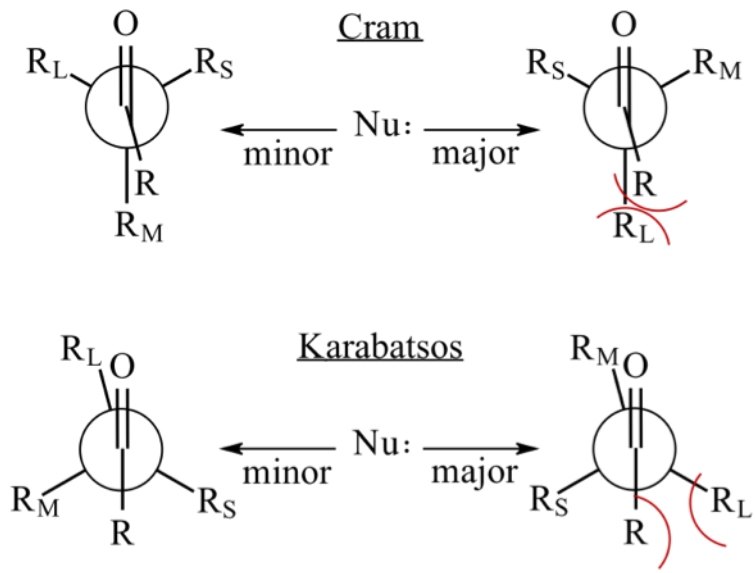

Figure 2.10: The Cram and Karabatsos asymmetric induction models. These transition states would theoretically decrease in diastereoselectivity with increasing size of R. This is not born out by experiment.[11]

2.1.3.3 Felkin postulates and resulting model

Felkin presents "a simple, internally consistent interpretation of the steric outcome of these reactions" for open-chain (acyclic) carbonyl compounds and cyclic ones as well.[8] He describes four postulates to set up the system and determine the lowest energy transition state, with the fourth postulate specific to cases where an electronegative substituent is attached to the α-carbon, forming a polar bond. This fourth postulate involving the polar case will be discussed later in the thesis. The first three postulates of this model are paraphrased from the paper as follows:

1. The transition states are in all cases reactant-like, although perhaps not as strictly reactant-like as proposed by Karabatsos.

2. Torsional/Pitzer strain at the transition state represents a substantial fraction of total strain in the molecule, even for a reactant-like transition state, where the degree of bonding is low. It is therefore essential for the transition state to be as staggered as possible. This can be accomplished by having the nucleophile approach in between two of the groups on the α-carbon. Eclipsed or half-eclipsed geometries should be avoided.

3. The most important steric interactions involve the nucleophile and the ketone's R group. Too much emphasis has been placed on minimizing steric repulsion at the carbonyl oxygen in the past.

By considering these 3 postulates, 6 staggered geometries are possible (Figure 2.11). Conformations denoted "A" yield the Felkin product (major product according to the Felkin model), while "B" conformations yield the anti-Felkin product. Conformation A1‡ is the most stable in terms of steric repulsion, followed by B1‡ and B2‡. In A1‡, the small group is staggered between (gauche to) the nucleophile and R group at the transition state. This causes the least amount of steric strain possible. The next most favoured transition state is B1‡, featuring gauche interactions between Nu, R, and R_M. Third comes B2‡, with a single gauche interaction between Nu and R_L, while A2‡, A3‡, and B3‡ feature gauche orientations between the R_L and Nu or R (or both) that are unstable.

If we inspect the most relevant structures in Figure 2.12 we can see that the most stable transition state, A1‡, will yield the major product. Increased selectivity towards A1‡ can be achieved by increasing the size of R_L or Nu as this will destabilize the B2‡ geometry with respect to A1‡. Another way the reaction can be made more selective is to increase the size of R. As R becomes larger, the steric repulsion between R and R_M in B1‡ will increase relative to A1‡, increasing selectivity towards A1‡. Some less straightforward effects can be observed when varying the size of R_M: increasing the size of R_M will cause strain in B1‡, but this simultaneously destabilizes transition state A1‡, so this will not af-

fect selectivity in a favourable way. An interesting observation is that as one increases the size of R_M, the more it resembles R_L, causing the difference in strain energy between A1‡ and B2‡ to decrease. In fact, if $R_M = R_L$, A1‡ would be energetically equal to B2‡ (this is always true in the non-polar case).

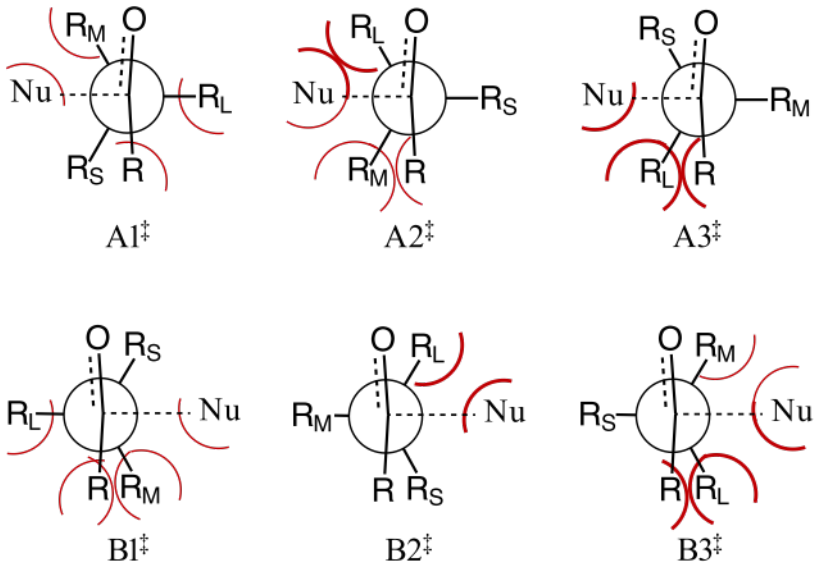

Figure 2.11: The possible staggered transition states as proposed by Felkin *et al.* Red curved lines are drawn to help qualitatively assess the amount of steric repulsion for each geometry. When R_S, R_M, and R_L are non-polar (alkyl) groups, A1‡ is the most stable. B1‡ and B2‡ follow in stability. The other three feature gauche interactions between Nu, R_L, and R that are strongly disfavoured.

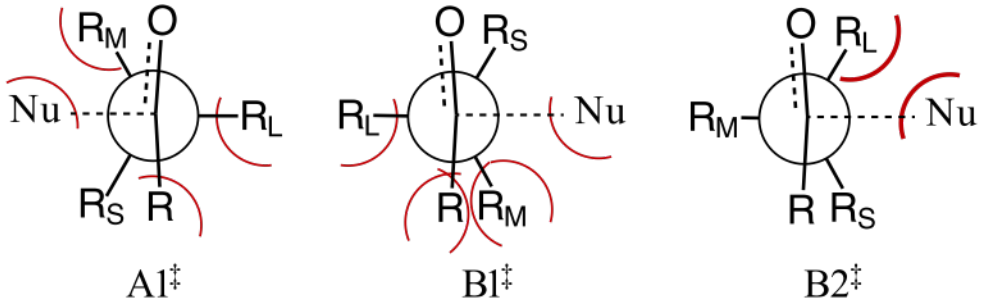

Figure 2.12: The most relevant transition state structures in Felkin's paper. "A" structures feature addition to one face of the carbonyl, while "B" structures add to the other face, resulting in the other product. A1‡ is the lowest energy transition state according to Felkin's postulates.

Table 2.2: Diastereoisomeric product ratios (F1/F2) resulting from $LiAlH_4$ reduction of ketones in Figure 2.13 (R_M = Me, R_S = Nu = H) in ether at 35 °C. In parentheses are the activation enthalpy differences ($\Delta\Delta H^{\ddagger}$). Table reproduced from results discussed by Cherest, Felkin, and Prudent.[8] R" = C_6H_5.

R_L	R = Me	R = Et	R = *i*-Pr	R = *t*-Bu
cyclohexyl	1.6 (-1.1)	2.0 (-1.1)	4.1 (-1.5)	1.6 (+0.1)
phenyl	1.8 (-1.0)	3.2 (-0.9)	5.0 (-0.3)	49 (-2.7)

The trend of increasing selectivity with increasing size of R can be observed in Figure 2.13 (the cyclohexyl case) for R = Me, Et, *i*-Pr. There is a significant drop in selectivity when R = *t*-Bu. This is thought by Felkin's group to be caused by strain between R and R_L, and since $B2^{\ddagger}$ features R_L at a farther distance from R than does the other two, $B2^{\ddagger}$ would be stabilized relative to the others (in spite of the proximity of R_L in $B2^{\ddagger}$ to Nu and O).

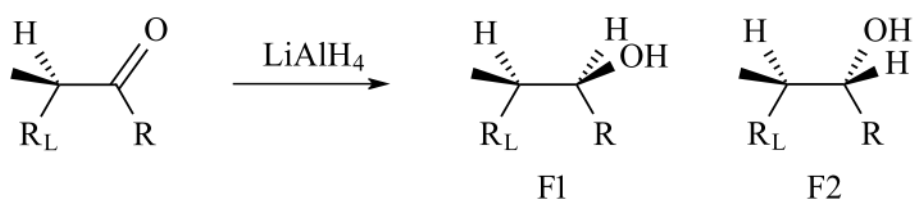

Figure 2.13: Reacting a chiral ketone with lithium aluminum hydride.

The last feature brought up in the paper that pertains to the non-polar case is the effect of changing the size of R_M on the stability of the relevant transition state, which can vary wildly depending on the nature of the other groups. As the size of R increases, larger R_M groups increase the strain in structure $B1^{\ddagger}$ (Figure 2.12). It has already been observed that in the non-polar case, R_M has little effect on the selectivity of $A1^{\ddagger}$.

An interesting feature of this model is observed when a polar R_L substituent is present. Increasing the size of R_M has an effect on the selectivity of the reaction, as the polar effects in $B2^{\ddagger}$ will be destabilizing relative to $A1^{\ddagger}$. This helps to account for a trend found in a series of hydride reductions of ketones performed by Cram and associates: "with R = *i*-Pr,

the [F1/F2] ratio increases from 5 when M = Me to 10 when M = *i*-Pr" (Figure 2.14).[12] This and other electronic consequences of this model will be discussed in section 2.2.2.

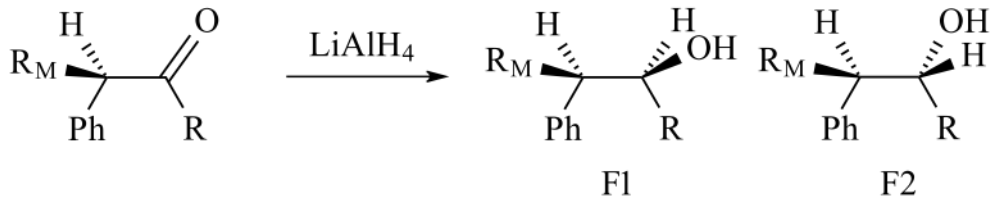

R_M	F1 / F2
Me	5.0
iPr	10.0

Figure 2.14: Diastereoisomer ratios (Felkin/Cram product to anti Felkin/anti Cram product) resulting from $LiAlH_4$ reduction in ether at 35° C (R_S = Nu = H). Results reproduced from Cram 1954.[12]

The Felkin model rationalizes some of the inconsistencies found in the Cram and Karabatsos models. The minimization of torsional strain and a nucleophilic trajectory approaching between the small and medium-sized groups yields a model that is more consistent with empirical evidence regarding how intramolecular interactions affect the diastereoselectivity of the model. This model is expected to reliably predict many acyclic and even simple cyclic reactions of this type.

2.1.4 Anh and Eisenstein's change to the Felkin model (Felkin-Anh, FA)

At this point, the majority of models to predict asymmetric induction have considered a limited number of conformations at the transition state, narrowed down using restrictions based on arguments involving various destabilizing noncovalent interactions. A paper by

Nguyen Trong Anh and Odile Eisenstein challenged this approach, claiming that no sufficient evidence had yet been provided to justify the disregard for multiple transition state geometries.[13] To verify if the elimination of certain transition state geometries was indeed justified, Anh and Eisenstein performed quantum mechanical calculations in which the single bond between the α-carbon and the carbonyl carbon (αC–CO) was rotated in 30° increments to yield 12 possible conformers for the reactant (Figure 2.15). Hydride (H^-) itself was chosen to represent the nucleophile and was placed on either face of the carbonyl 1.5 Å perpendicularly to yield 24 potential transition states, 12 for each diastereomeric product. The energies of these 24 geometries were computed using Hartree-Fock ab initio fixed potential scans with the STO-3G basis set.[14] The energies of hydride adding to 2-chloropropanal were plotted in Figure I, III, and IV of their original paper (see Figure 2.15), while a plot of 2-methylbutanal is featured in Figure II.

For each plot, the solid line corresponds to the transition state leading to the major product as the αC–CO bond is rotated, while the hashed line corresponds to the transition state leading to the minor product according to Cornforth's rule (discussed in section 2.2, a polar analogue to Cram's rule). Figure 2.15 shows that the geometries presented by Cornforth do not correspond at all to the lowest energy transition state geometry that corresponds to the products, and would be less than 0.1% in a Boltzmann equilibrium. The Felkin transition states are much lower in energy and resemble more closely the lowest energy transition state calculated. Anh rationalizes the Felkin transition state energies on an electronic basis, noting that the H^- anion and the Cl group are separated as much as possible in these geometries.

In Figure 2.15 II, the electron-withdrawing Cl was substituted with a non-polar Et group (2-methylbutanal) to investigate how the reaction proceeds with a non-polar substituent. Again it was found that Felkin's transition states were close to the transition state geome-

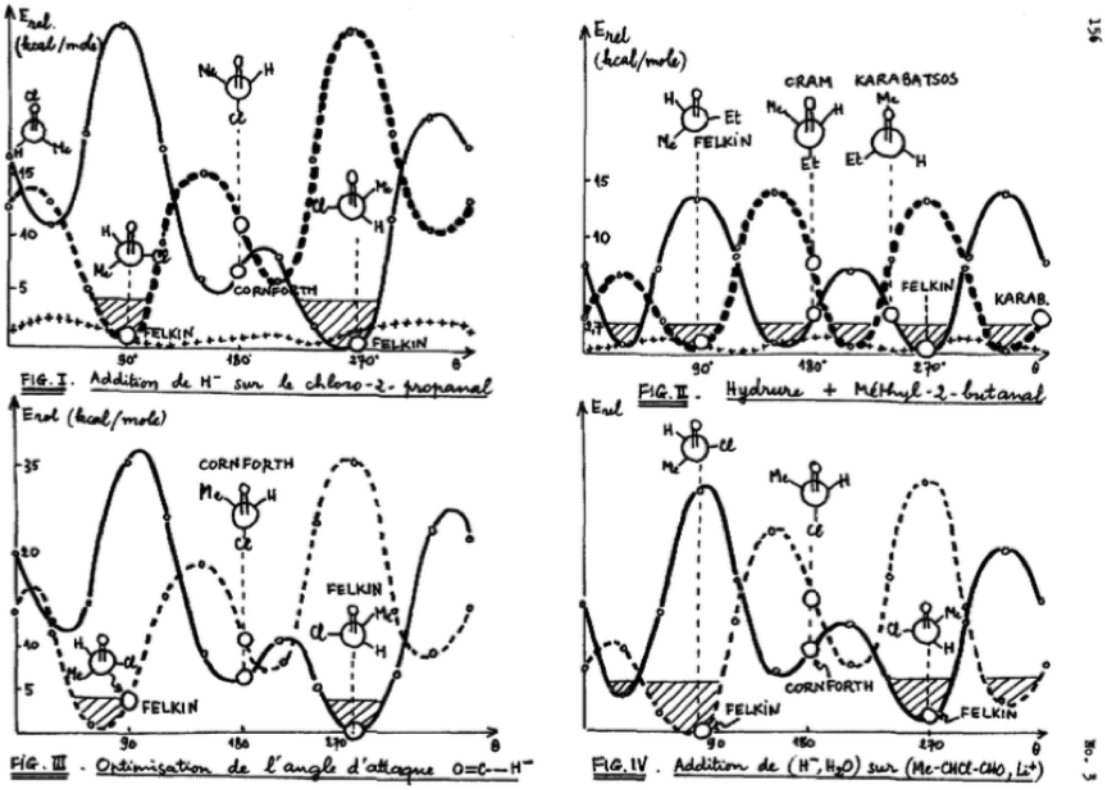

Figure 2.15: The results of the calculations of Anh and Eisenstein as presented in their paper.[13]

tries that were calculated to be lowest in energy, while the Cram and Karabatsos transition states were much higher in energy (+2.7 kcal/mol). Figure 2.15 IV addresses solvation in which the same calculatons were performed in the presence of one specific water molecule solvating H^-. The angle of attack is assumed perpendicular to the carbonyl. Figure 2.15 III incorporates the work of Bürgi and Dunitz (Appendix A3) regarding the trajectory of the incoming nucleophile. When the O=C$\cdots$H$^-$ angle of attack is set at an angle wider than 90° (~107° depending on the reaction), the transition state energy decreases[15] Adjusting the angle of attack on the Felkin model in this way led to the lowest energy transition state calculated in the study, resulting in an adjustment to the Felkin model referred to as the Felkin-Anh (FA) model (Figure 2.16).

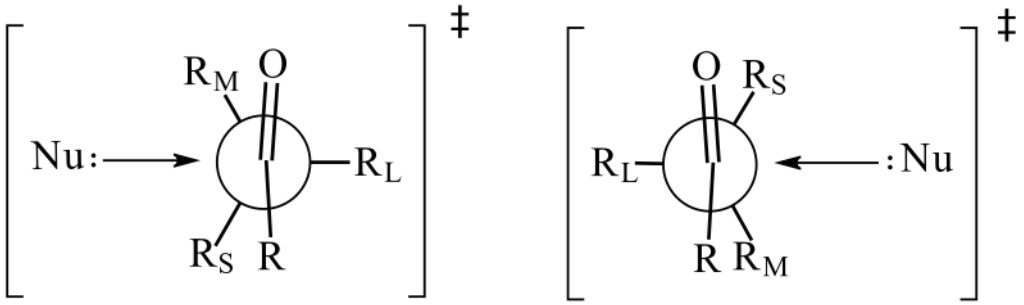

Figure 2.16: The Felkin model (left) and the optimization by Anh (right) inspired by the work of Bürgi and Dunitz.[15] The angle of attack of the nucleophile along the Nu···C=O angle widened from 90° to ~107°.

Figures 2.15 I, III, and IV were described as qualitatively interchangeable. In each case, the Felkin transition state energies were the lowest of the three models being compared. The authors conclude that the only significant transition states are from Felkin, and the geometries are better optimized in the Felkin-Anh model. The lower energy of the Felkin-Anh transition states were attributed to favorable secondary orbital interactions at the transition state of the hydride addition. During the nucleophilic addition, the filled hydride 1s orbital overlaps directly with the $\pi^*_{C1=O}$ orbital to form the σ_{C1-H} orbital of the product. If the hydride adds anti to the C2–R_L bond, favorable secondary orbital interactions be-

tween the nascent σ_{C1-H} orbital and the neighboring $\sigma^*_{C2-R_L}$ orbital were proposed. This hyperconjugation would be much weaker if the hydride were to add *syn* to the R_L group (Figure 2.17).

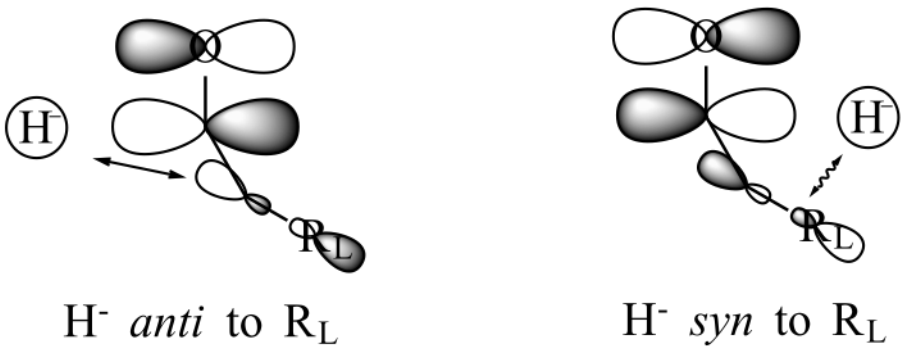

Figure 2.17: Overlap between the filled hydride 1s orbital and the $\pi^*_{C1=O}$ orbital forms the σ_{C1-H} orbital of the product. Favorable secondary orbital interactions between the hydride 1s orbital and the neighboring $\sigma^*_{C2-R_L}$ orbital at the transition state is possible only if the hydride adds anti to the R_L group. Figure reproduced from Anh, Eisenstein 1976.[13]

It appears that a model for asymmetric nucleophilic addition is more accurate when considering antiperiplanarity of R_L to the incoming nucleophile over minimizing torsional strain. When aligning R_L in this manner, the torsional strain is reasonably well minimized. The FA model still carries weight in the literature and will be referred to extensively later on in this thesis.

2.1.5 Wintner (1987) (bent bond theory)

In his *J. Chem. Educ.* paper, Wintner calls for more inclusion of the Slater/Pauling bent bond representation for double bonds in introductory level organic chemistry classes to explain more clearly stereoelectronic effects and reactivity in organic chemistry.[16] He also uses the bent bond model to interpret asymmetric induction in the addition to α-chiral carbonyl compounds. His model uses the following two postulates:

1. The nucleophile trajectory is fixed and approaches in-line with the larger lobe of the antibonding $\tau^*_{C=O}$ orbital, which helps rationalize the wide angle of approach when compared to the σ/π model (employed by Felkin to rationalize an approach of the nucleophile perpendicular to the carbonyl). This is loosely consistent with the wide angle of nucleophilic trajectory established previously by Bürgi and Dunitz, although this will give an angle of attack approaching 120° which is wider than any typical nucleophilic trajectory specified by Bürgi and Dunitz.[15]

2. The lowest energy transition state will yield the major product in accordance with the Curtin Hammett principle.[17] The geometry Wintner chooses to demonstrate the τ bonding model eclipses the R_M and R_L with the τ-bonds of the carbonyl. This is not the most stable ground state geometry, but does correspond to a staggered geometry in the product. This agrees with the contributions of Anh and Houk relating to the antiperiplanarity of Nu to R_L and the staggering of the substituents on the α-carbon with respect to the products.[13,18] Two structures are in contention as the most likely to be the lowest energy transition state, one for each product with the attack between the R_S and R_M groups, antiperiplanar to the R_L group. It is worth noting that the transition state will feature both partial single and partial double bonded character, so the eclipsing of the τ-bonds may not be as disfavoured as it appears when drawn this way.

The model ends up looking very similar to the FA model (Figure 2.18).

2.1.6 BBAH model

In 2011, Ghislain and Pierre Deslongchamps published the first of a series of papers describing how organic structures and chemical reactivity can be interpreted in an intuitive way by their bent bond/antiperiplanar hypothesis (BBAH).[19–23] The BBAH is based on the bent bond model for unsaturated systems and supplements it with modern stereoelec-

tronic concepts for interpreting a wide range of organic properties and reactivities. In their first article, they present an alternative model for diastereoselective nucleophilic additions to α-chiral carbonyls based on the BBAH. Their diastereoselectivity model places the α-chiral carbonyl compound in a conformation that naturally staggers the bent bonds of the carbonyl with respect to the α-carbon substituents (an eclipsed conformation in σ/π parlance, see Figure 2.6). Of the three possible staggered rotamers, two of them orient the hydrogen on the α-carbon antiperiplanar to one of the C=O bent bonds, allowing for $\sigma_{\mathrm{CH}} \rightarrow \tau^*_{\mathrm{C=O}}$ hyperconjugation to occur (left of Figure 2.19). As a result, that particular bent bond is electron-enriched and less apt to undergo opening by a nucleophile so it is the opposing bent bond that undergoes S_N2-like addition. The final BBAH-based model shown on the right of Figure 2.19 considers the trajectory of nucleophilic attack and has the nucleophile approaching R_M at the transition state (the other rotamer would have the nucleophile approaching the larger R_L group at the transition state). Overall the model predicts the same diastereomeric product outcome as the other models.

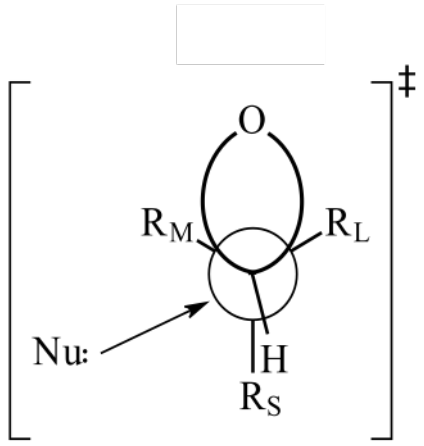

Figure 2.18: Wintner model. Eclipsing of the τ and σ bonds is disfavoured in the ground state. This eclipsing is not expected to adversely affect the energy of the transition state, as the oxygen gains significant single bond character at this point.

2.2 Polar models for asymmetric induction

The following section summarizes the most influential models in the literature of 1-2 asymmetric induction on carbonyls where one of the three bonds on the stereogenic α-carbon is polar.

2.2.1 Cornforth (1959)

In a paper that focused on the stereoselective synthesis of olefins, J. Cornforth, R. Cornforth, and Mathew addressed the electronic effects found to influence the asymmetric induction of reactions with carbonyl compounds, as the production of α-chlorohydrins (a reaction involving asymmetric induction) is the first of three steps for forming the desired alkene in their paper.[24] Cornforth *et al.* were looking for an alternative to Wittig and Schöllkopf's method for olefin synthesis, as it yielded a mixture of stereoisomers. Corey had shown previously that liquid 2-chlorocyclohexanone exists entirely in the axial chlorine conformer (Figure 2.20).[25–27] Electrostatic repulsion between the dipoles of C–Cl and C=O were thought to destabilize the equatorial conformer. For reactions on acyclic systems, if a Cl group were to be placed on the α-carbon, perhaps this interaction would force the molecule in a geometry that would predominantly yield one of the two chlorohydrin

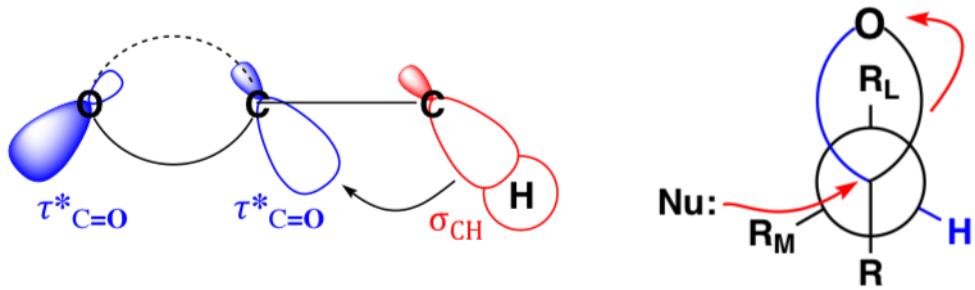

Figure 2.19: BBAH model. Left: hyperconjugation between the $\sigma_{C\text{–}H}$ orbital of the C–R_S bond (R_S = H) and the antiperiplanar $\tau^*_{C=O}$ orbital increases electron density of the τ bond. Right: the opposing (i.e. weaker) τ bond is broken during nucleophilic attack.

isomers when reacted with a nucleophilic agent (Grignard or organolithium reagent).

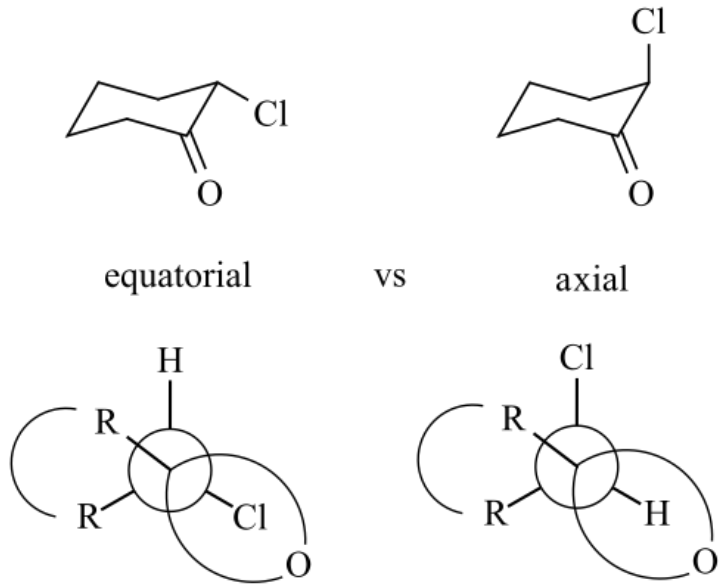

Figure 2.20: Two geometries of 2-chlorocyclohexanone (corresponding Newman projections of bent bond models shown below).

The resulting Cornforth model (Figure 2.21) positioned the polar X group anti to the C=O group based on minimizing dipole-dipole repulsion. They argue that the electrophilic activity of the carbonyl depends on the extent of C=O charge separation and that minimizing the net dipole (by placing Cl anti to the carbonyl) helps maximize the C=O charge separation by drawing more electron density away from the carbonyl carbon. This looks quite similar to Cram's rule if one substitutes the X group for the R_L group. The diastereoselectivity depends on the difference in size between R_S and R_M, as the side that is less hindered will be the major product.

2.2.2 Polar Felkin Model

The 4th postulate in Felkin's model will be discusssed in this section as it discusses the case where a polar substituent is located on the α-carbon:

4. Polar groups: If an electronegative substituent, X, is present on the α-carbon (replace R_M, or R_L with X), transition states that separate Nu and X will be stabilized by polar effects.[8]

Cram's rule is a poor predictor of diastereoselectivity on substrates that bear an electronegative polar group at position R_M.[24] The polar Felkin model accounts for this, as the polar effects will stabilize B2‡, the geometry that maximizes separation between the nucleophile and the electronegative R_M group. This shifts the selectivity toward the anti-Cram product. B1‡ and A1‡ are expected to be greatly destabilized in this case owing to the close proximity of R_M, Nu, and O (Figure 2.22).

If the electronegative group is R_L, the selectivity towards the Cram/Felkin product in-

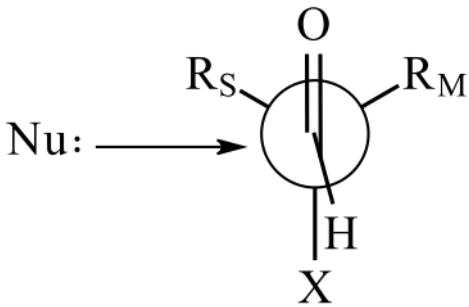

Figure 2.21: Cornforth's model for asymmetric induction. To minimize the net dipole of the carbonyl substrate, the polar X group is oriented anti to the oxygen. The nucleophile then adds to the less hindered side featuring the smaller of R_S and R_M.

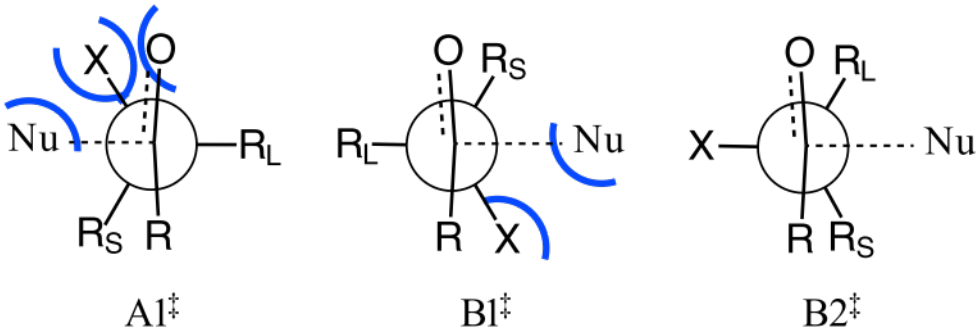

Figure 2.22: Destabilizing interactions between electronegative groups in the Felkin model when R_M is electronegative (R_M = X). In this case, transition state B2‡ is favored.

Table 2.3: Diastereoisomeric product ratios resulting from $LiAlH_4$ reduction of the ketone in Figure 2.13 (R_M = Me, R_S = Nu = H) in ether at 35° C. In parentheses are the activation enthalpy differences ($\Delta\Delta H^{\ddagger}$). Table reproduced from results reported in Felkin 1968.[8] R" = C_6H_5.

R_L	R = Me	R = Et	R = *i*-Pr	R = *t*-Bu
cyclohexyl	1.6 (-1.1)	2.0 (-1.1)	4.1 (-1.5)	1.6 (+0.1)
phenyl	1.8 (-1.0)	3.2 (-0.9)	5.0 (-0.3)	49 (-2.7)

creases (the opposite result when compared to an electronegative R_M group). This is observed in Table 2.3, where the more electronegative phenyl group increases the selectivity of the reaciton. This effect is increased with bulkier R groups, owing to the increased steric strain in transition state B1‡, and is especially noticable when R = *t*-Bu. Increasing the size of an electronegative R_L should increase strain in transition state B2‡, causing a slight increase in selectivity for the expected product.

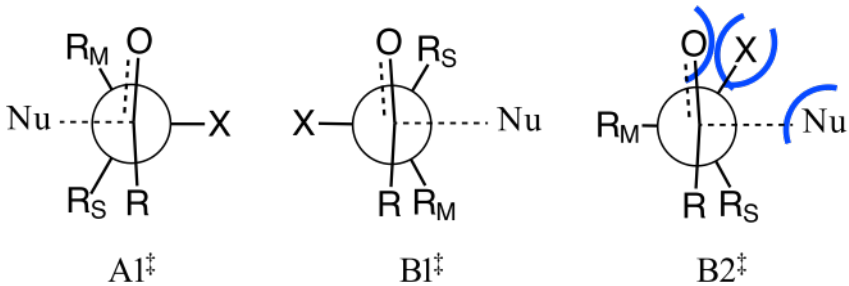

Figure 2.23: Destabilizing interactions between electronegative groups in the Felkin model when R_L is electronegative (R_L = X). It can be observed that reaction pathway A gains further preference over pathway B.

Felkin's model for heteroatom-substituted α-chiral aldehydes is one step closer to understanding the mechanics of nucleophilic additions to these compounds. It offers insight into the ways that a polar group can influence the stereoselectivity of the reaction, and how the selectivity can be affected differently when the polar group is either a medium or a large group.

The polar Felkin-Anh model (PFA) adjusts the geometry of the polar Felkin model so that it incorporates the reaction trajectories discussed by Bürgi and Dunitz.[15] The wider attack angle (O=C$\cdots$Nu angle 90° –> ~107°) lowers the calculated energy of the system and is therefore expected to be a more powerful predictive model. This change in angle does not significantly affect the interactions at the transition state in a qualitative sense, but does relieve tosional strain at the transition state.

2.2.3 Evans' modified Cornforth Model (2003)

In 2003, the David Evans group proposed a modified Cornforth model (MC) that was adjusted to account for the torsional effects at the transition state by staggering substituents at the transition state (as in the Polar Felkin-Anh (PFA) model).[28] Instead of having the electronegative group (C–X) antiperiplanar to the forming bond to participate in a hyperconjugative effect as in PFA, the MC model prioritizes dipole minimization between C–X and C=O, placing the electronegative group gauche to the incoming nucleophile (Figure 2.24).

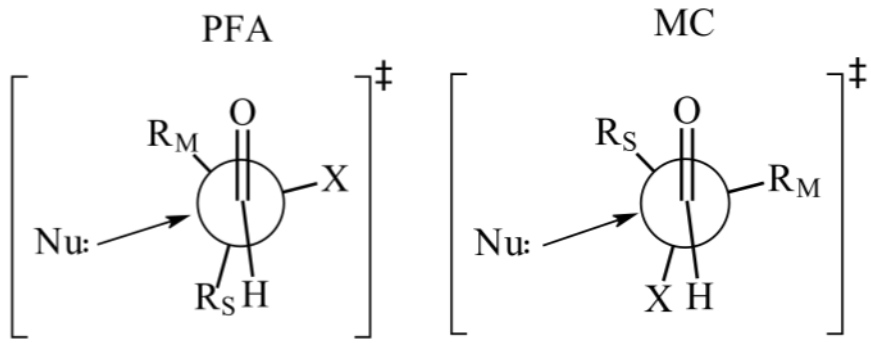

Figure 2.24: Comparing the polar Felkin-Anh (PFA) (left) and modified Cornforth (MC) (right) models.

While the PFA model has been widely adopted to predict 1,2-asymmetric induction of α-heteroatom-substituted aldehydes, Evans shows the potential for the MC model to pre-

dict the outcomes of reactions where the nucleophile imposes a conformational restriction on the α-stereocenter at the transition state. This type of restriction is cleverly demonstrated in a series of aldol reactions involving the addition of substituted enolates to α-hetereoatom-substituted aldehydes. Depending on whether the PFA or MC model was used, reacting the aldehyde with a *Z*-enolate or an *E*-enolate would be predicted to impose a highly destabilizing *syn*-pentane conformation at the transition state (Figure 2.25). The PFA model predicts that the *E*-enolate will give superior selectivity towards the 3,4-anti product, as the *Z*-enolate experiences a *syn*-pentane interaction at the transition state, hampering diastereoselectivity for this isomer. In contrast, the MC model predicts better selectivity from the *Z*-enolate because it avoids *syn*-pentane interactions at the transition state.

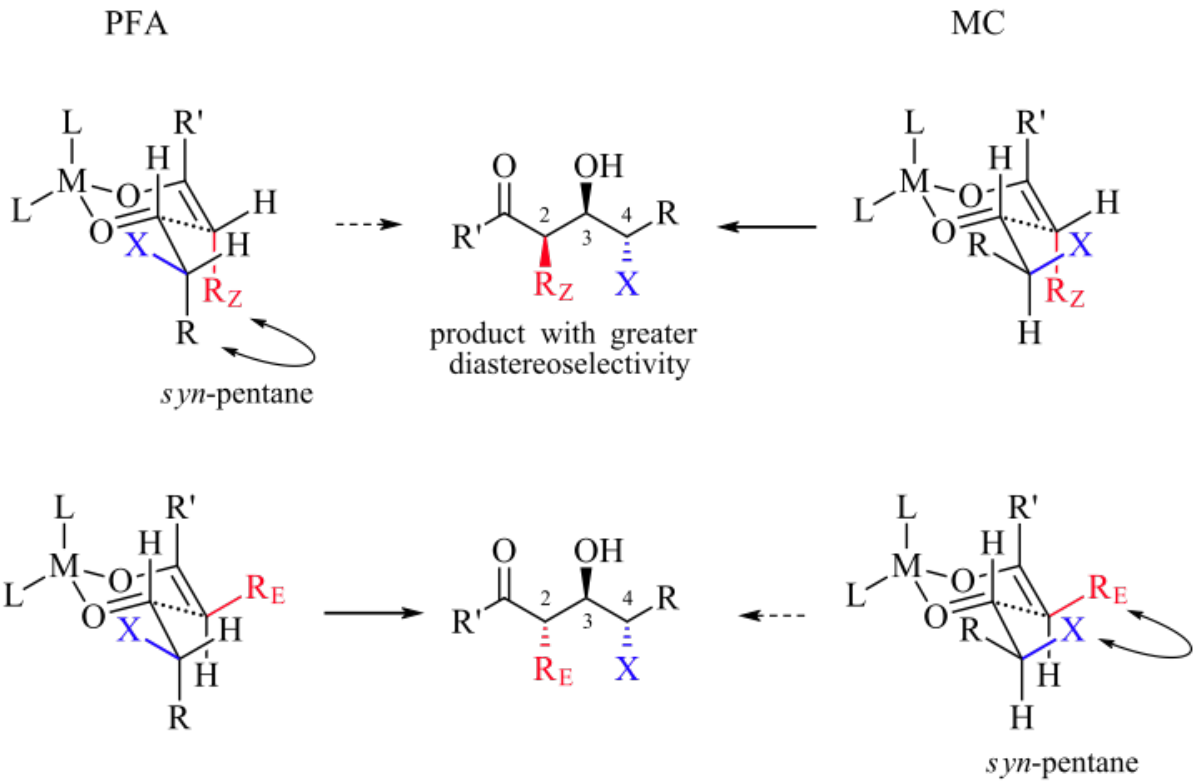

Figure 2.25: Comparing transition states resulting from the PFA and MC models. Figure reproduced from Evans 2003.[28]

It was found that the *Z*-enolate yielded greater diastereoselectivity, indicating that the MC model is potentially more viable for predicting reactions involving pericyclic chair transition states. Although the reaction being investigated in this thesis is an acyclic reaction, the MC model will be investigated to verify its predictive power on acyclic systems.

Chapter 3

Methodology

3.1 Choosing a model reaction

It was important to select a model system that was as simple as possible while exhibiting all the key features of diastereoselective nucleophilic addition to carbonyl compounds. A simple system enables the reaction trajectories to be isolated and studied with the fewest possible operating factors and the least computational demand. The features required are as follows: 1) a simple nucleophile archetype capable of adding to a carbonyl group, and 2) a carbonyl group exhibiting diastereotopic faces due to 3) an adjacent carbon (α-carbon) stereocenter.

3.1.1 Choice of nucleophile

3.1.1.1 Hydride anion

The simplest nucleophile that could have been chosen would have been the hydride anion. Nucleophilic hydride reagents such as $NaBH_4$ and $LiAlH_4$ are typically used for carbonyl reduction reactions but present many complications for modelling as their exact reaction trajectory may not be easily predicted and their countercations can coordinate to the car-

bonyl groups. Hydride anion itself would not be a suitable nucleophile to model because it is very different from the actual reagents ($NaBH_4$, $LiAlH_4$) and is a very poor nucleophile because its lone pair resides in a low-lying 1s orbital. Furthermore, hydride addition to an aldehyde would produce a 1° alcohol, so no stereogenic center would be created during the reaction.

3.1.1.2 Hydroxide anion

The hydroxide anion was not chosen because its attack trajectory would also have to be considered. Indeed, the hydroxyl oxygen is sp_3 hybridized, so it cannot attack at a 180° H–O····C angle as it approaches the carbonyl carbon due to the position of the lone pairs of electrons. Numerous H–O····C attack angles would have to be investigated, complicating the overall computational study. The more important issue, however, is that hydroxide addition to any carbonyl group produces a hydrate (after protonation) that bears two OH groups and is thereby not generating a chiral center. A further complication is that hydrate formation is always reversible and, in most cases, endergonic such that product formation would be under thermodynamic control. The ratio of the diastereomeric products in reactions under thermodynamic conditions are determined by relative energies of the products, not the activation energies as in kinetic reactions (see Appendix A.2). Therefore hydroxide was not selected as a nucleophile for the computational investigation of the previously discussed diastereoselectivity models.

3.1.1.3 Organometallic reagents

Grignard reagents and organolithium compounds are common strong nucleophiles used in aldehyde addition reactions. These reagents were not chosen as a nucleophile in the model system because the presence of the metal introduces many complicated variables to

the system. Including metals can considerably increase the computational demands of the model system, as the increased number of electrons and degrees of freedom in the system take longer to calculate. Organometallic reagents can also form aggregates in solution so the actual nucleophilic species may not be well characterized. Their metal component can also coordinate to the carbonyl and participate actively in the addition reaction, forming a cyclic transition state that completely changes which interactions predominate at the transition state of the reaction.

3.1.1.4 Cyanide anion

Cyanide anion (referred from this point on simply as cyanide) was chosen as the model nucleophile as it addresses all the issues described for the previous reagents. Addition of cyanide to an α-chiral aldehyde generates a new stereogenic center resulting in two cyanohydrin diastereomers upon protonation of the oxyanion. The cyanide carbon is sp hybridized and retains that hybridization upon nucleophilic addition, resulting in a 180 ° N=C····C angle of attack that greatly narrows down the possible reaction trajectories. The role of the sodium or potassium cation in the typical cyanide source (NaCN or KCN) is also believed to be much less critical than those in the organometallic reagents because Na^+/K^+ are poor Lewis acids, which form much weaker coordination complexes. As a result, these metals are not believed to interact much with the carbonyl group of the aldehyde reactants during nucleophilic addition.

Even though the cyanide addition reaction is technically a reversible reaction, the conditions required for the cyanohydrin product to collapse back to aldehyde and cyanide are fairly demanding. For example, heating a cyanohydrin in aqueous acid or base can, in principle, collapse the cyanohydrin via either acid or base-catalyzed mechanisms. However, treating cyanohydrins under such conditions usually converts the nitrile group, first to a

primary amide and then to a carboxylic acid, with no apparent collapse of the cyanohydrin. So the cyanohydrin reaction is not so easily reversible as it is unlikely to survive the reaction conditions that facilitate hydrolysis of the nitrile group. Thus the addition of cyanide to α-chiral aldehydes can be considered at least pseudo-kinetic and seems a reasonable model system for this computational study. As a result, the computational characterization of the reaction transition states should correlate with the diastereomeric ratio of the cyanohydrin products.

3.1.2 Choice of carbonyl substrate

The model carbonyl compounds were chosen to be aldehydes rather than ketones as the reactions proceed more quickly via the less sterically hindered aldehydes. Cyanohydrin addition to ketones is not unheard of, but as the ketone gets sterically bulkier, the reaction becomes slow and less practical. An added benefit is that using an aldehyde will reduce the number of atoms involved in the calculations using quantum mechanics (QM).

3.1.3 Choice of substituents on α-carbon

The final structural variables of the system to be selected involve the three substituents attached to the α-carbon (marked Small, Medium, and Large). For the small and medium sized substituents, hydrogen and methyl were used due to their small size and prevalence in reactions in the literature.[29] The large substituent was varied from a phenyl group (commonly found in the literature – allows comparison to similar reactions) to a *t*-butyl group to see the effects on the diastereoselectivity of the reactions with increasing steric bulk. Karabatsos discussed this structure, 2,3,3-trimethylbutanal, in his paper although no experiments were performed on it. Finally, a chlorine group was chosen to investigate the influence of a polar bond on diastereoselectivity, as was used in Anh and Eisenstein's

paper.[13]

3.1.4 Solvation

The inclusion of solvation in the calculations was considered, although it was ultimately decided that it was not worthwhile to include in the calculations.

3.1.4.1 Explicit solvation:

The most useful form of solvation to include would be explicit solvation, although the increased computational demand and the ambiguity of how many and where to place the explicit solvent molecules made explicit solvation too complicated to include in the calculations. There was a significant amount of difficulty with getting the calculations that involve only the aldehyde and cyanide to resolve to a true transition state, so the increased degrees of freedom would make the calculations more difficult to resolve.

3.1.4.2 Implicit solvation:

A choice that would be more computationally economic would be implicit solvation, where solvation of the system would be accounted for by adding a term in the quantum calculations that account for solvation instead of including explicit solvent molecules in the system. While this would result in a slightly more quantitative model of the system, there would not be a significant qualitative difference in the potential energy surface.

3.1.5 Model summary

In summary, the model reaction chosen for this thesis was the addition of cyanide to simple α-chiral aldehydes, corresponding to the initial step of the cyanohydrin reaction. This

system should prove sufficient to investigate the influence of different α-substituents on diastereoselectivity. Very few examples of asymmetric cyanide additions to carbonyl compounds can be found in the literature except for some enzyme catalyzed or organocatalyzed cases.[30–32] However, the computational study of cyanide addition to α-chiral aldehydes constitutes a simple molecular system unencumbered by several, potentially complicating factors.

3.2 Performing calculations

3.2.1 Description of the software used in this study

3.2.1.1 MOE

The Molecular Operating Environment is a drug discovery software package that features advanced molecular modeling capabilities.[33] MOE is based on SVL (scientific vector language) allowing for new methods and functionality to be integrated into the system via user-written SVL programming. MOE was used to carry out preliminary geometry optimizations by molecular mechanics, to generate input files for QM calculations, and for geometric analysis of computational output.

3.2.1.2 GI-MOE

The Gaussian Interface for MOE is a SVL program developed by the Deslongchamps group for interfacing MOE with the Gaussian 09.[34] GI-MOE was used to generate various input files for Gaussian, including multi-structure files such as those required for carrying out potential scans. GI-MOE was also used to convert Gaussian output into MOE-savvy databases for data viewing and analysis.

3.2.1.3 Gaussian 09

Gaussian version 09 (G09) is a QM program available to UNB researchers via ACENET, a consortium of post-secondary institutions in Atlantic Canada.[35] All G09 calculations were performed on ACENET via the GI-MOE interface to MOE.

3.2.1.4 Matlab

Matlab is a numerical computing environment and programming language for performing various mathematical operations.[36] The curves from the potential energy scans were plotted using Matlab.

3.2.2 Computational methods

3.2.2.1 Inital modelling

Molecules were initially modelled in MOE and geometry optimized via molecular mechanics using the MMFF94x force field and gas-phase conditions. These structures were then used as input for subsequent QM calculations in G09. All QM calculations were performed in G09 using density functional theory (DFT) and the B3LYP functional. In general the 6-31++G** basis set was used for the calculations as well as the 6-31g(d) basis set for some simpler, preliminary calculations. All calculations were performed in the gas phase.

3.2.2.2 Geometry optimizations

Geometry optimizations via DFT were performed for the ground state of the reactants and products, as well as for the transition states. Ground states and transition state geometry

optimizations require different calculations. It is relatively simple to optimize the geometry of a ground state, as the calculation searches for the lowest energy point in all directions of the potential energy surface. This is similar to a marble rolling down the edge of a bowl to the lowest point in the center (Figure 3.1).

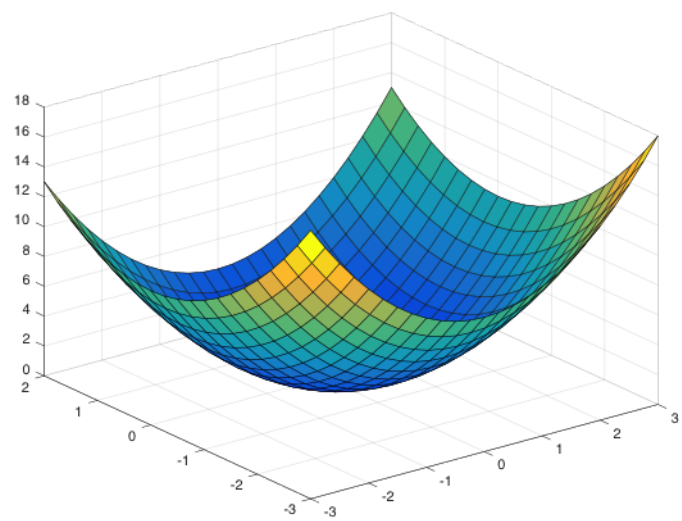

Figure 3.1: A paraboloid with a minimum at (0, 0, 0).

For transition state optimization, a saddle point must be found where the energy is at a maximum along one and only one direction (i.e.dimension) of the potential energy surface, finding the highest energy point from reactants to products. However, the energy must be at a minimum in all other directions, i.e. all bond lengths and angles must be optimized to achieve stability at the transition state. The potential energy surface will look like a hyperbolic paraboloid in this case. Reaction coordinates will normally proceed from the reactants to the products along the lowest energy path, with the transition state being the saddle point (Figure 3.2).

3.2.2.3 Fixed vs. Relaxed potential scans

In this thesis, the potential energy scans were obtained via relaxed potential scans. A simpler method for obtaining a potential scan would be the fixed potential scan. A fixed potential scan is obtained by choosing one (or more) dihedral angles of a molecule or set of molecules and rotating the angle incrementally, calculating the energy of that point each time. This method was employed by Anh and Eisenstein.

What makes the relaxed potential scan more advantageous over the fixed potential scan is that each time a rotation occurs, all other bond distances and angles are allowed to adjust in order to achieve a less strained and more realistic depiction of the system under the specified parameters. A relaxed potential scan allows the potential energy scan to more closely resemble the true energy surface. Since this thesis is an attempt to get a clearer picture on the predictive power of the various models in the literature, relaxed potential scans, while more resource intensive, were chosen as the method to obtain the various potential energy surfaces required in this thesis.

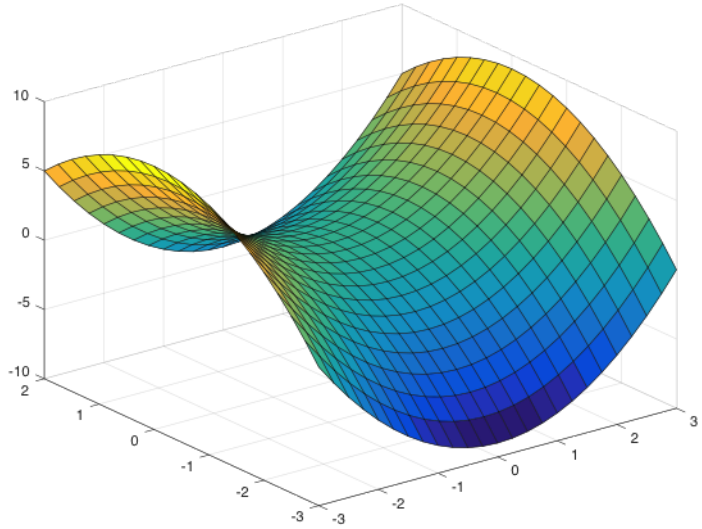

Figure 3.2: A hyperbolic paraboloid with a saddle point at (0, 0, 0).

3.2.3 Setting up input files

3.2.3.1 Relaxed potential scans of ground states

Relaxed potential energy scans of ground states were performed through the following general method:

1. Generate a molecule in MOE and geometry optimize with MMFF94x
2. Re-optimize the geometry using G09 (B3LYP/6-31++G**)
3. Using GI-MOE, setup relaxed potential scan, rotating about the O=C–C–RL dihedral angle in 10° increments over 360° (RL denotes the Large substituent)
4. Submit the relaxed potential scan calculation to G09 on ACENET
5. Import G09 output with GI-MOE and interpret data using MOE

3.2.3.2 Relaxed potential scans of transition states

Relaxed potential energy scans of transition states were performed through the following general method:

1. Generate a trial transition state geometry in MOE with MMFF94:
   (i) The nucleophile is placed ~2 Å away from the aldehyde carbon
   (ii) The bond angle for the trajectory of the nucleophile (O–C–Nu) is set to ~110° while bisecting the carbonyl plane
   (iii) The aldehyde is manually pyramidalized to somewhat emulate a geometry between that of the planar reactant and the tetrahedral products

2. Geometry optimize the transition state using the Berny method in G09 (DFT/B3LYP).[37]

3. Verify validity of transition state by geometry inspection and reviewing eigenvalues from the G09 output.

4. Using GI-MOE, setup relaxed transition state potential scan, rotating about the O=C–C–RL dihedral angle in 10° increments over 360°

5. Submit the relaxed transition state potential scan calculation to G09. Verify validity of transition state by geometry and eigenvalues from the G09 output

6. Import G09 output with GI-MOE and interpret data using MOE.

3.2.4 Interpretation of output files

It is important to be able to recognize when the transition state calculations produce the correct output. Visual inspection of the output structure allows the user to assess qualitatively if the transition state obtained corresponds to the correct reaction, i.e. that the correct bonds are being broken/formed along the desired reaction pathway. In addition, analysis of the G09 output determines whether a true transition state was identified. Frequency calculations performed during G09 optimization compute the force constants of the system and the resulting vibrational frequencies.[37] If the frequency calculations yield zero imaginary frequencies, then the geometry is that of a ground state, i.e. the 1st derivatives of all the dimensions of the potential energy hypersurface are zero. If one imaginary frequency is obtained, the geometry is a transition state, i.e. all the 1st derivatives of the potential energy hypersurface are zero except for one, which is negative. More than one imaginary frequency is indicative of a calculation that did not optimize to a transition or ground state geometry for our model system.

Once the output files were compiled using GI-MOE, we could import the zero-point energy corrected energies to any data processing software. Matlab was used to plot the data comparing dihedral angle rotation to the energy of the system, using spline interpolation to generate a line connecting the points of each potential energy scan. This generated a curve that simplifies visual inspection of the plots.

The data plots generated were used to compare the geometries of the various models from the literature. Once the models were represented on the plots, they could be compared to see which model best represents the lowest energy transition state geometry.

Chapter 4

Results & Discussion

4.1 Introductory remarks

The following section reports the results of the relaxed potential scans for the cyanide addition to three aldehyde compounds referred to as the *t*-butyl, phenyl and chloro compounds throughout this chapter (Figure 4.1). Each aldehyde had the absolute stereochemistry shown (note that both the *t*-butyl and phenyl compound have the *R* configuration whereas the chloro has the *S* configuration due to the higher priority of chlorine in the Cahn-Ingold-Prelog rules). For each aldehyde, calculations were carried out for the two possible diastereomeric outcomes of the reaction, one corresponding to the addition of CN^- to the *re* face of the aldehyde and one for the addition to the *si* face.

4.2 Potential scan graphs

The results of the potential energy scans are graphed in Figure 4.2, Figure 4.3, Figure 4.4. Each data point in the graphs represents the energy of the reaction transitions states located by B3LYP calculation at each fixed rotation of the O=C–C–R_L dihedral angle while allowing all other structural parameters to be geometry-optimized. The graphs represent

the relative energies of these transition states as the O=C–C–R_L dihedral angle was rotated systematically in 10° increments. When dihedral angles that imposed a large amount of strain on the compounds occurred, the calculations would sometimes not optimize to a true transition state geometry. This is why there are not always 36 data points for each potential scan. Spline interpolation was used to generate a continuous line to estimate the energies of the potential energy surface. The spline interpolation had some difficulty with the terminal ends of the graph, so these parts drawn by hand. Upon inspection of the graphs, it is nevertheless clearly possible to infer what kinds of interactions are dictating the overall energy of the transition state.

4.3 Discussion

4.3.1 Non-polar substrates (R_L = *t*-Bu, Ph)

4.3.1.1 Cyanide trajectory

The two nonpolar aldehydes that feature a *t*-Bu or a Ph group as the R_L substituent are qualitatively very similar. They each feature three energy minima and maxima for both

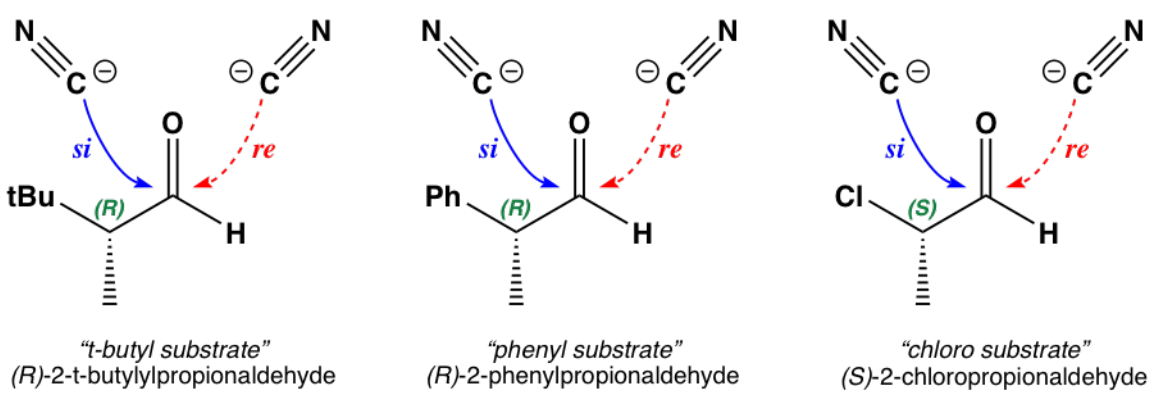

Figure 4.1: Addition of cyanide to the *re* and *si* faces of the *t*-butyl, phenyl, and chloro compounds.

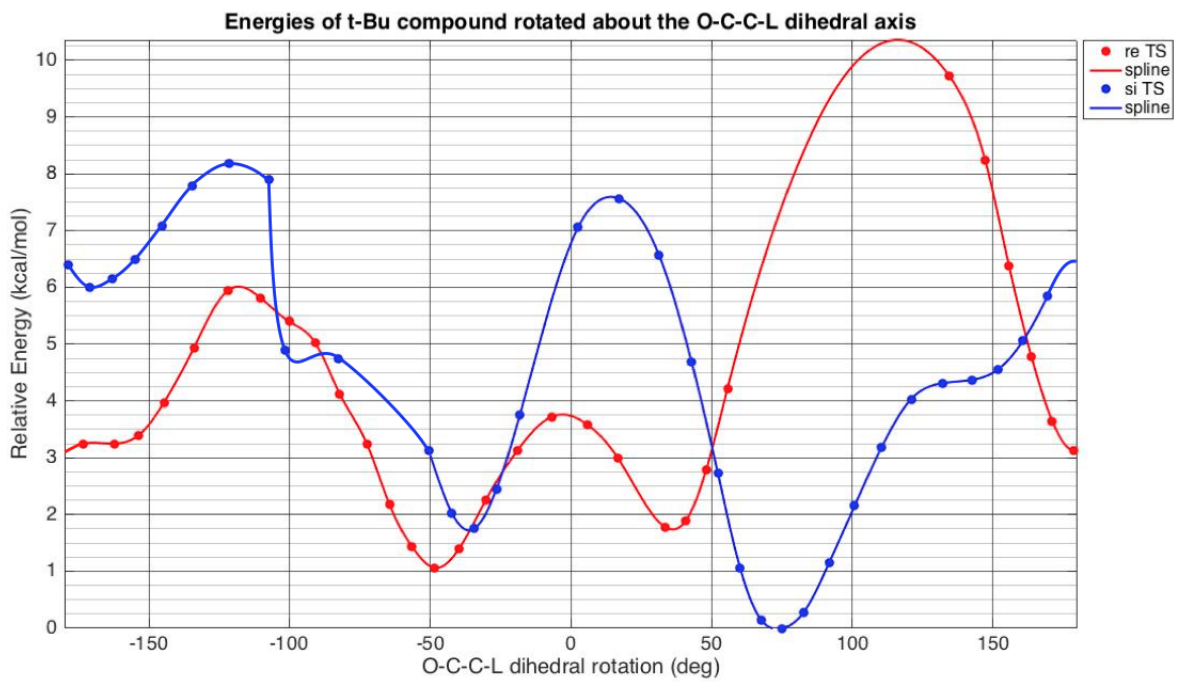

Figure 4.2: PES of *t*-butyl compound. Points on the graph refer to calculated energies, while lines that connect the points were generated using spline interpolation and hand drawing. 0° occurs when C=O and αC–R_L are *syn* to each other. O=C–C–L = O=C–C–R_L.

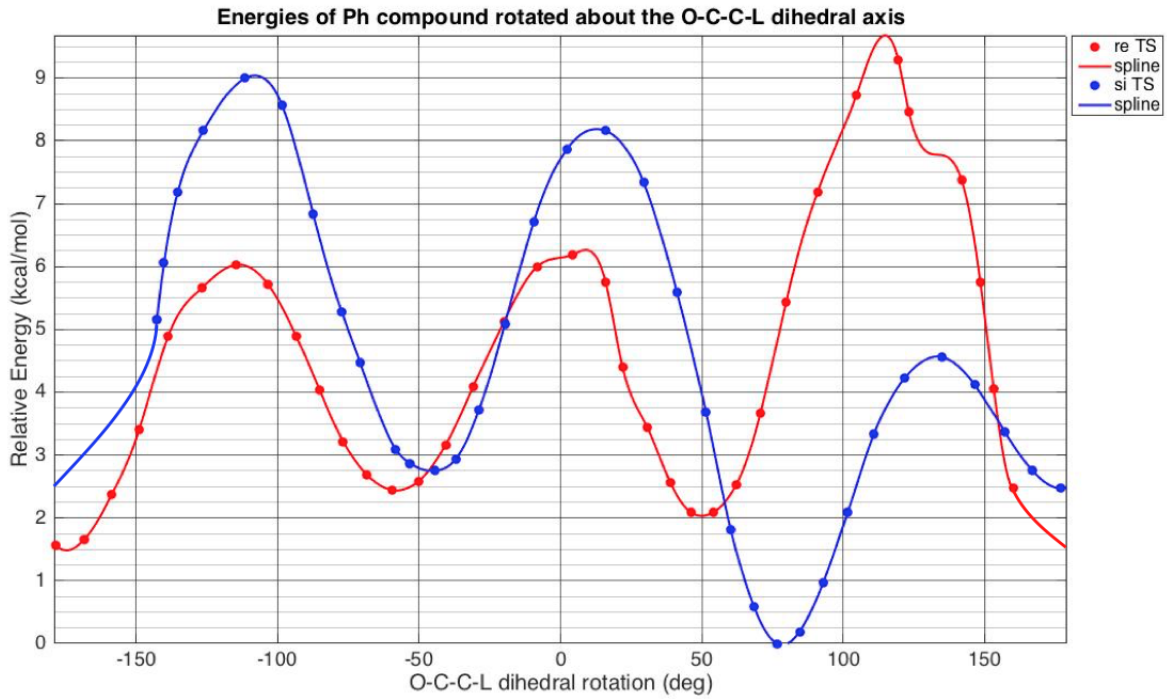

Figure 4.3: PES of phenyl compound. Points on the graph refer to calculated energies, while lines that connect the points were generated using spline interpolation and hand drawing. 0° occurs when C=O and αC–R_L are *syn* to each other. O=C–C–L = O=C–C–R_L.

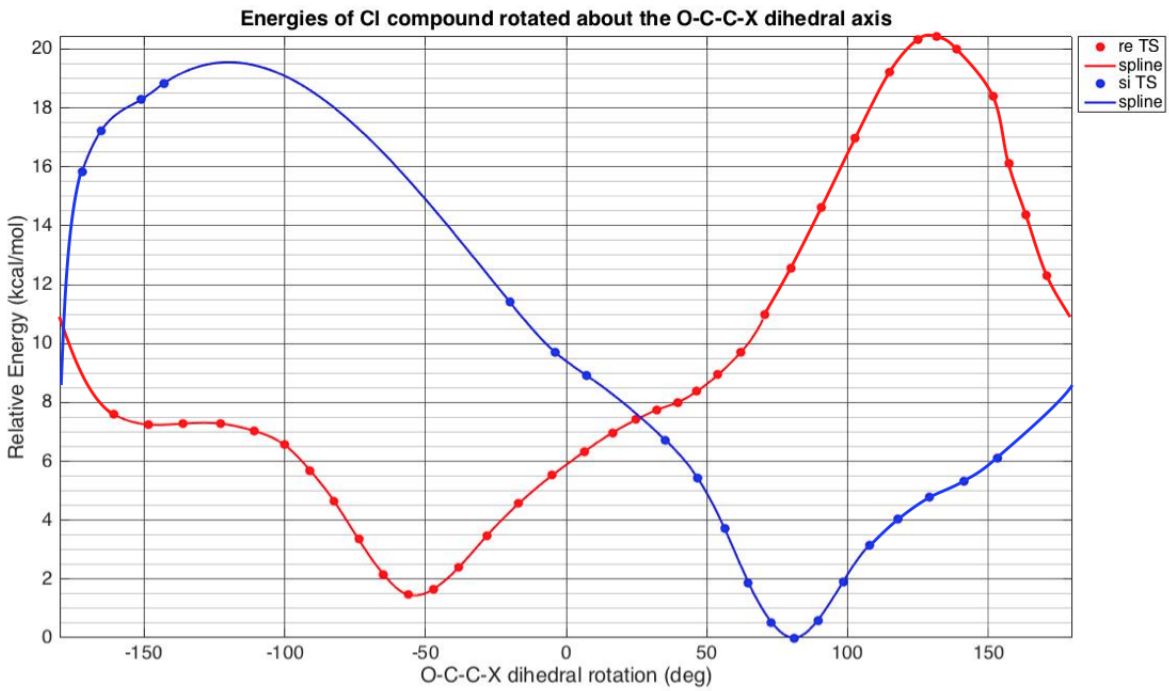

Figure 4.4: PES of chloro compound. Points on the graph refer to calculated energies, while lines that connect the points were generated using spline interpolation and hand drawing. ”X” refers to chlorine atom. 0° occurs when C=O and αC–R_L are *syn* to each other.

the *re* and *si* facial additions. The minima are found when the incoming cyanide nucleophile is staggered between two of the substituents on the α-carbon, while the maxima (~9 kcal/mol higher) are found when the incoming cyanide eclipses one of the substituents on the α-carbon stereocenter. As the nucleophile approaches, the Nu–O=C angles were wider than 90°, as predicted by Bürgi and Dunitz. The Nu–O=C angles varied from ~110 to 113° and the lowest energy transition states in each case exhibited an angle of ~112.5°.

4.3.1.2 Prediction of diastereoselectivity for *t*-butyl compound

Analysis of the two potential energy scans for the *t*-butyl compound (Figure 4.5) reveals that the lowest energy transition state corresponds to cyanide addition from the *si* face of the aldehyde, the latter having a conformational O=C–C–R_L dihedral angle of ~75°. When the reaction occurs in this geometry, it is ~1.1 kcal/mol lower in energy than the next lowest transition state geometry, which corresponds to the lowest energy geometry for addition to the *re* face. These two lowest energy transition states feature the incoming cyanide staggered between the small and medium sized groups, minimizing steric hindrance at the transition state. Thus one must consider this to be the dominant transition state geometry for addition to the *t*-butyl compound.

The geometry of the best *si* addition features the *t*-butyl group antiperiplanar to the incoming CN– group. The methyl group is located on the other side of the carbonyl than the *t*-butyl group, and the hydrogen is situated anti to the carbonyl. The geometry of the best *re* addition appears quite similar to the *si* addition although the methyl and hydrogen have swapped places with respect to the carbonyl. Overall, the computational results indicate diastereoselectivity in favor of addition to the *si* face, which corresponds to what is predicted by the models described in Chapter 2. Thus, the minimum for *si* addition (O=C–C–R_L dihedral angle ~75°) can be considered to be the most kinetically favoured

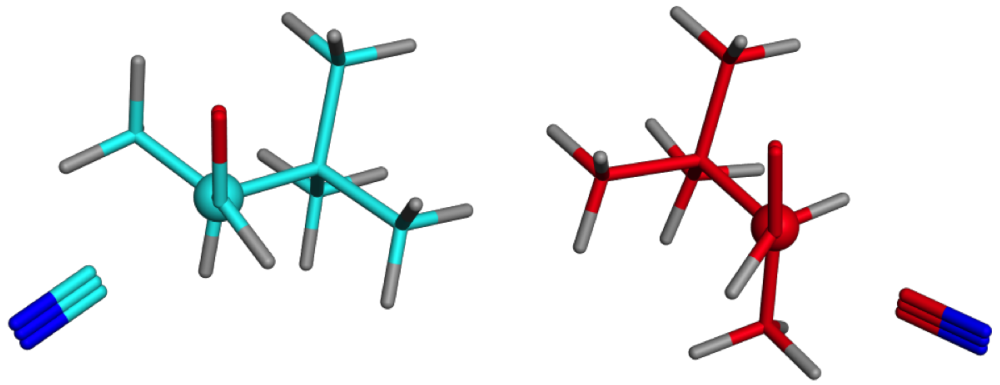

Figure 4.5: Lowest energy transition state geometries for cyanide addition to the *si* face (left) and *re* face (right) of the *t*-butyl compound. Addition to the *si* face was preferred by 1.1 kcal/mol.

transition state for the addition of cyanide to (*R*)-2-*t*-butylpropionaldehyde. A comparison of this transition state geometry against the other diastereoselectivity models will be discussed in section 4.3.3.3.

4.3.1.3 Prediction of diastereoselectivity for the phenyl compound

Analysis of the two potential energy scans for the phenyl compound (Figure 4.6) reveals that the lowest energy transition state corresponds to cyanide addition from the *si* face of the aldehyde, the latter having a conformational O=C–C–R_L dihedral angle of ~75°. When the reaction occurs in this geometry, it is ~1.6 kcal/mol lower in energy than the next lowest transition state geometry, which corresponds to the lowest energy geometry for addition to the *re* face. The *si* addition features the incoming cyanide staggered between the small and medium sized groups as in the case with the *t*-butyl substrate. The *re* addition features the incoming cyanide staggered between the medium and large sized groups, which was not expected based on the predictions made in the literature. Some other interaction must be occurring that supersedes the stability conferred by orienting the CN^- group between the smaller groups.

4.3.2 Polar substrate

4.3.2.1 General observations

The potential scans for the polar aldehyde, (*S*)-2-chloropropionaldehyde, appear qualitatively different from the two nonpolar ones. As shown in Figure 4.4, there is one clear minimum energy transition state, and one very maximum (~19 kcal/mol) for both the *re* and *si* addition. The potential scan results support the large dipolar electrostatic contribution to the transition state energies due to the polar C–Cl bond. It seems that the electrostatic effects (i.e. dipole-dipole interactions) overshadow any steric effects as one

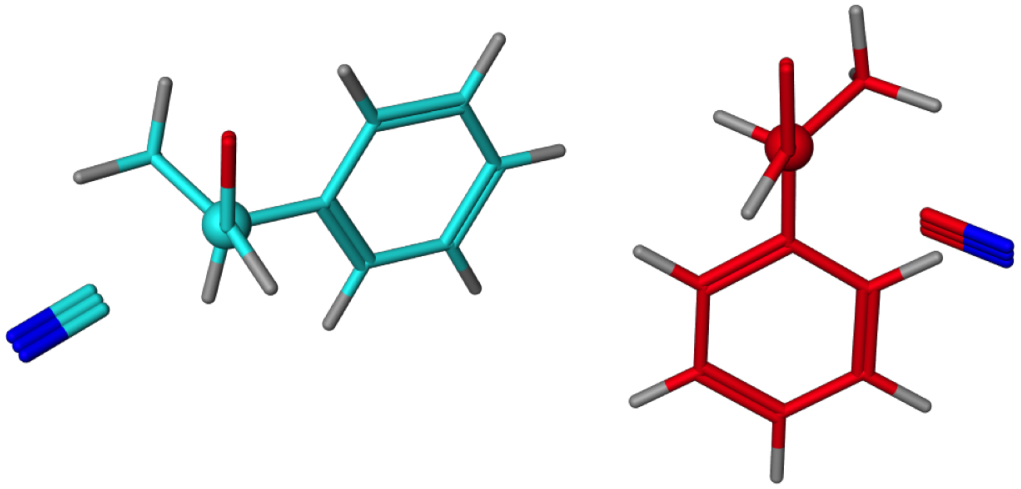

Figure 4.6: Lowest energy transition state geometries for cyanide addition to the *si* face (left) and *re* face (right) of the phenyl compound. Addition to the *si* face was preferred by 1.6 kcal/mol.

no longer sees the three peaks that are typically attributed to eclipsed/staggered conformations as the O=C–C–Cl is rotated. One can dismiss the possibility that the Cl group is large enough to impart significant steric interactions with the other atoms of the aldehyde during bond rotation, so the dipole-dipole interactions must ultimately be dominant.

4.3.2.2 Prediction of diastereoselectivity for the chloro compound

As seen in Figure 4.7, addition to the *si* face of the *S* enantiomer is preferred by ~1.5 kcal/mol, comparable to the energy difference observed in the nonpolar systems. The next lowest energy addition corresponds to *re* addition, similar to the *t*-butyl compound. The lowest energy minimum corresponds to that for *si* face addition at a O=C–C–Cl dihedral angle of ~80° where the cyanide trajectory again staggers between the small and medium sized groups, and is anti to the chlorine substituent. This slightly wider angle could result from electronic interactions between the Cl and the O that would prefer more distance between these two electronegative atoms.

4.3.3 Comparative analysis against other models

To assess the predictive diastereoselectivity of the various models from the literature, Figure 4.8, their respective O=C–C–R_L dihedral angles can be taken from the geometries specified by each model to be mapped directly onto the three PES plots.

4.3.3.1 Dihedral angle predictions for non-polar compounds

The geometries from the literature will be quickly summarized here in order to illustrate how their respective dihedral angles will be mapped to the potential energy scans:

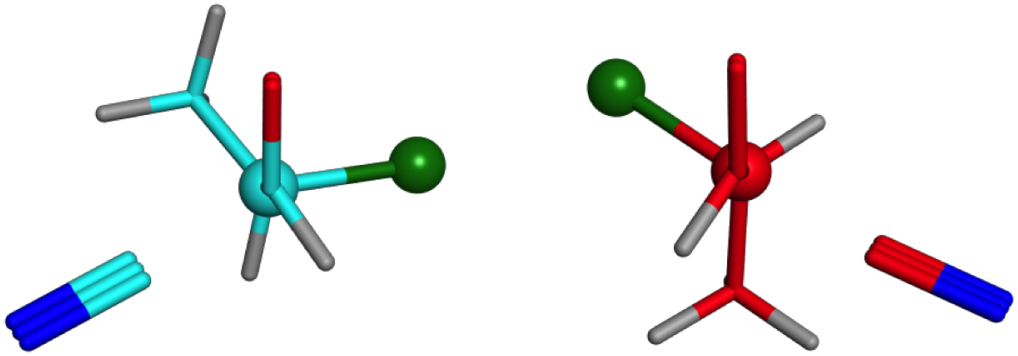

Figure 4.7: Lowest energy transition state geometries for cyanide addition to the *si* face (left) and *re* face (right) of the chloro compound. Chlorine shown in dark green. Addition to the *si* face was preferred by 1.5 kcal/mol.

Cram - 180°: The large group is anti to the carbonyl to minimize steric strain between O and R_L.

Karabatsos - 120°: The large group is staggered with respect to the carbonyl to minimize steric strain between R and R_L.

Felkin - 90°: The large group is set perpendicular to the carbonyl to minimize Pitzer strain and for Nu to overlap with the $\pi^*_{C–O}$ orbital.

Felkin-Anh - ~73°: (assuming 107° Bürgi-Dunitz angle of nucleophile addition, 180 - 107 = 73).[38] The large group is set antiperiplanar to the incoming nucleophile.

Wintner - ~68.5°: (180 - ((120+103)/2) = 68.5) A compromise between 1) the large group eclipsing τ bond for a favourable τ^* interaction (120°) and 2) the large group being set antiperiplanar to the incoming nucleophile (103°).[16,39]

BBAH - 0° : The large group eclipses the carbonyl to allow hyperconjugation between the C–H bonding orbital ($\sigma_{C–H}$) and one of the C=O antibonding orbitals ($\tau^*_{C–O}$).

4.3.3.2 Dihedral angle predictions for polar compounds

The geometries from the polar literature, Figure 4.9, will be quickly summarized here in order to illustrate how their respective dihedral angles will be mapped to the potential energy scans:

Cornforth - 180° : The polar group is oriented anti to the carbonyl to minimize the net dipole.

PFA - ~73° : The polar group is oriented antiperiplanar to the incoming nucleophile to maximize favourable overlap of their corresponding orbitals.

Evans' Revised Cornforth - -150°: The polar group is slightly offset from an anti position to the carbonyl to minimize both Pitzer stain and the net dipole.

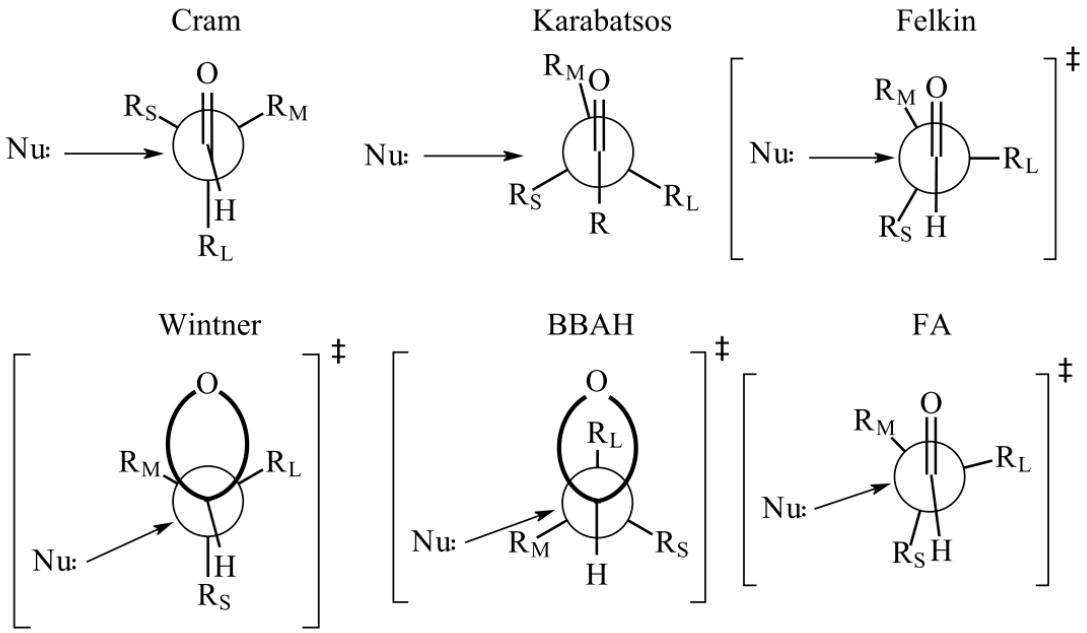

Figure 4.8: The various nonpolar predictive models that will be mapped to the PES plots.

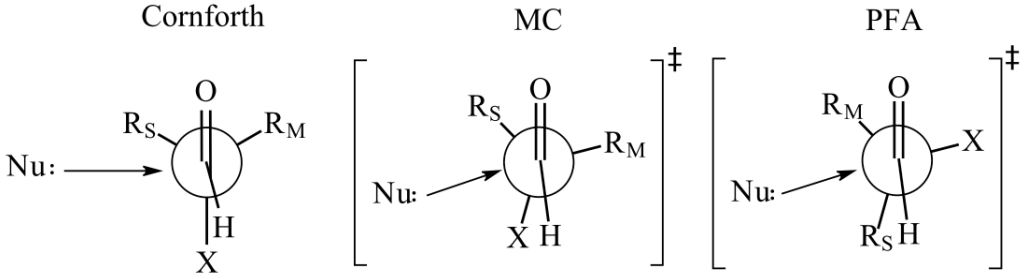

Figure 4.9: The various polar predictive models that will be mapped to the PES plots. Some nonpolar models will also be plotted to verify their ability to predict the outcome of the reaction.

4.3.3.3 Potential scan graphs updated with literature models

The three PES can now be updated to show where these dihedral angles correspond on the plots (Figures 4.10, 4.11, 4.12).

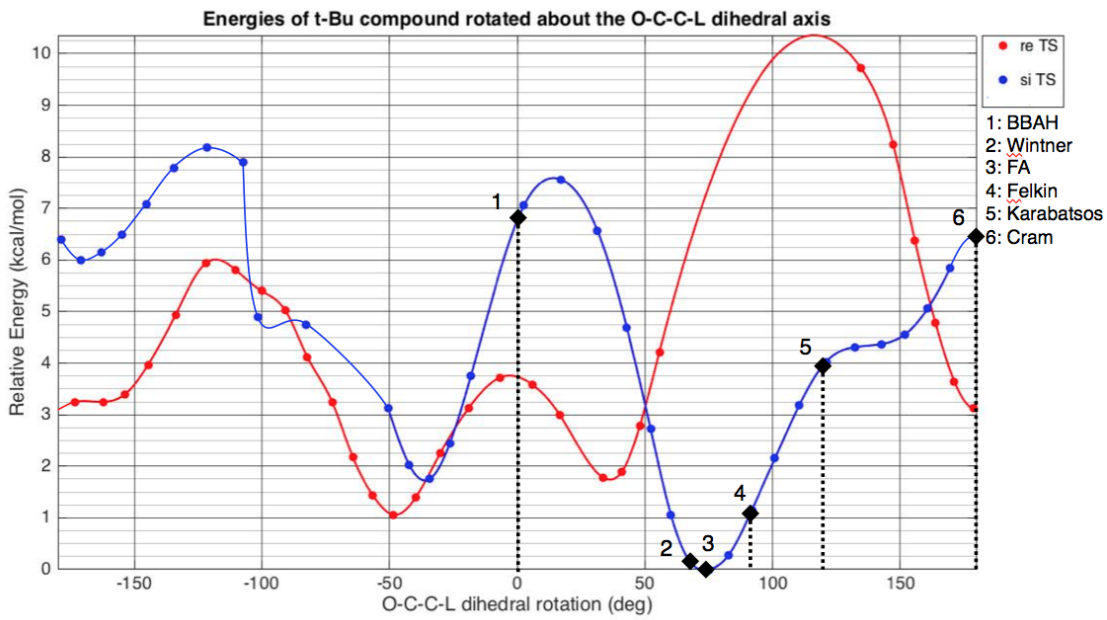

Figure 4.10: PES of *t*-butyl compound. Points on the graph refer to calculated energies, while lines that connect the points were generated using spline interpolation and hand drawing. 0° occurs when C=O and αC–R_L are *syn* to each other. O=C–C–L = O=C–C–R_L.

It is clear that, as various iterations of the predictive models were devised, they converged more closely to the transition state geometries found in this computational study (Cram —> Karabatsos —> Felkin —> FA). The models that map the closest to the global minimum transition state energy are the FA and the Wintner models. This gives an interesting result that a model that uses σ/π bonds and one that uses τ bonds are comparable in their predictive power for the reaction.

When looking at the polar case, we can see similar results. Models that consider stabilization from placing the heteroatom antiperiplanar to the incoming nucleophile correspond

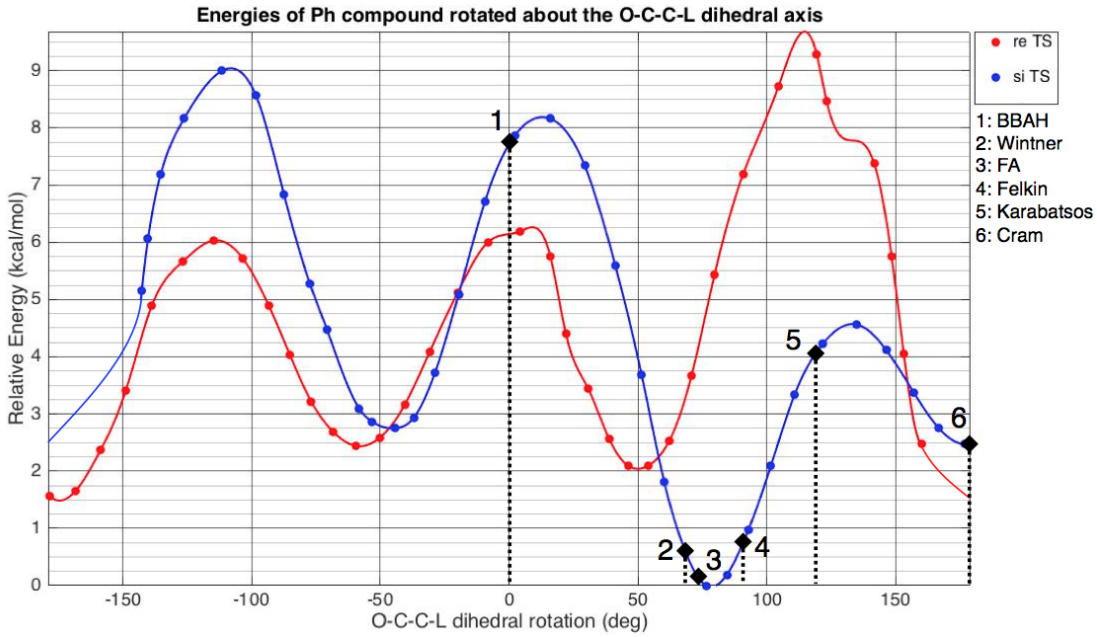

Figure 4.11: PES of phenyl compound. Points on the graph refer to calculated energies, while lines that connect the points were generated using spline interpolation and hand drawing. 0° occurs when C=O and αC–R_L are *syn* to each other. O=C–C–L = O=C–C–R_L.

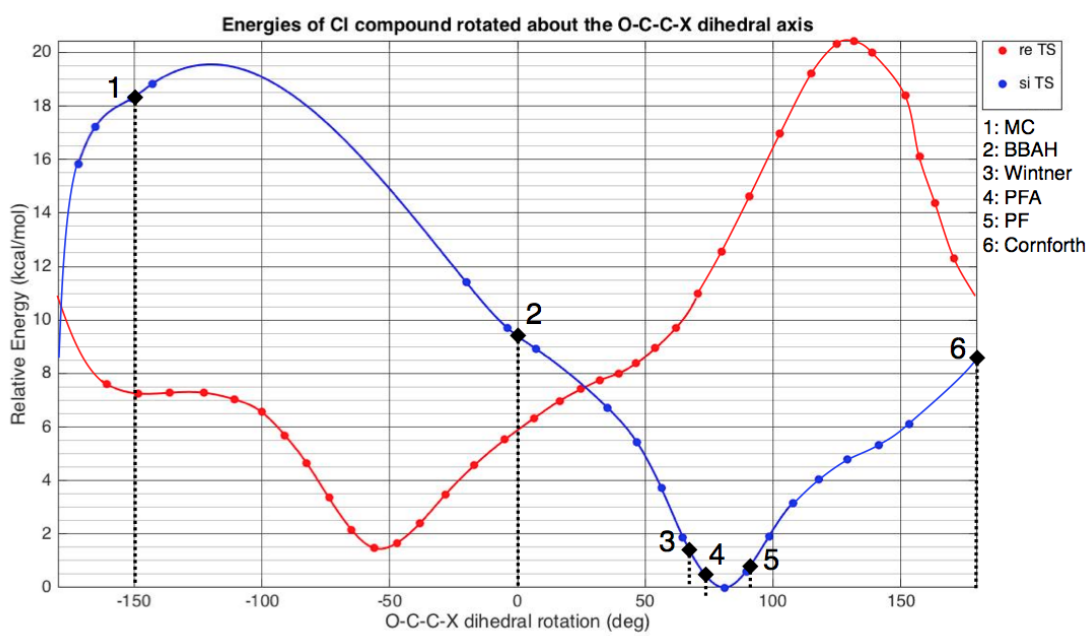

Figure 4.12: PES of chloro compound. Points on the graph refer to calculated energies, while lines that connect the points were generated using spline interpolation and hand drawing. X = Cl. 0° occurs when C=O and αC–R_L are *syn* to each other.

more closely to the computed transition state geometries which, by their nature, incorporate electrostatic interactions.

Chapter 5

Conclusions

Asymmetric induction models are used daily by organic chemists to aid them in their synthetic endeavours. Until now, a definitive investigation using high-level computation to test the validity of these models had never been conducted. Using relaxed potential energy scans allows for an investigation at a higher resolution than data obtained via fixed potential scans, as has been done in the past. The results of this study answer the remaining questions with respect to the validity of these commonly used models.

Based on the potential energy scans, the models that most accurately predict the lowest energy transition states are the Felkin-Anh and the Winter models and their polar analogues, while the other models are unable to do so. The geometric requirements of those two models are very similar, differing only in the localized orbital construct for the carbonyl group. Thus, it is safe to conclude that the important energetic factors that contribute to diastereoselective reactions are of the type that are discussed in these two models.

From the FA model, minimization of torsional/Pitzer strain and the antiperiplanarity between the Nu and the R_L/X group are clearly important, as these features are present in each low energy transition state.

From the Wintner model, the alignment of the $\tau^*_{C\text{-}O}$ orbital with the trajectory of the incoming nucleophile explains why a wider nucleophilic trajectory is preferred over a 90° trajectory that would align well with a $\pi^*_{C=O}$ orbital. A strong argument can be made for the use of bent bonds to more clearly picture what is happening mechanistically with the reaction.

BBAH, while stereoelectronically correct, does not consider the steric effects between the incipient nucleophile and the carbonyl substrate at the transition state. The interactions with the nucleophile are evidently very crucial to the mechanics of this reaction.

Bibliography

[1] D. J. Cram and F. A. A. Elhafez, "Studies in Stereochemistry. X. The Rule of "Steric Control of Asymmetric Induction" in the Syntheses of Acyclic Systems," *Journal of the American Chemical Society*, vol. 74, pp. 5828–35, Dec. 1952.

[2] D. J. Cram and K. R. Kopecky, "Studies in Stereochemistry. XXX. Models for Steric Control of Asymmetric Induction," *Journal of the American Chemical Society*, vol. 81, pp. 2748–2755, June 1959.

[3] G. J. Karabatsos, "Asymmetric induction. A model for additions to carbonyls directly bonded to asymmetric carbons," *Journal of the American Chemical Society*, vol. 89, no. 6, pp. 1367–1371, 1967.

[4] G. J. Karabatsos and N. Hsi, "Structural Studies by Nuclear Magnetic Resonance. X. Conformations of Aliphatic Aldehydes," *Journal of the American Chemical Society*, vol. 87, no. 13, pp. 2864–70, 1965.

[5] E. Hückel *Z. Phys.*, no. 60, p. 423, 1930.

[6] L. Pauling *Journal of the American Chemical Society*, no. 53, p. 1367, 1931.

[7] J. C. Slater *Phys. Rev.*, no. 37, p. 481, 1931.

[8] H. Felkin, M. Cherest, and N. Prudent, "Torsional strain involving partial bonds. The stereochemistry of the lithium aluminium hydride reduction of some simple open-chain ketones," *Tetrahedron letters*, vol. 9, no. 18, pp. 2199–2204, 1968.

[9] M. Cherest and H. Felkin, "Torsional Strain Involving Partial Bonds. The Steric Course of the Reaction Between Allyl Magnesium Bromide and 4-*t*-Butyl-Cyclohexanone," *Tetrahedron Letters*, no. 18, pp. 2205–08, 1968.

[10] A. Kamernitzky and A. Akhrem, "The stereochemistry of reactions of nucleophilic addition to the carbonyl group of cyclic ketones," *Tetrahedron*, vol. 18, pp. 705–750, Jan. 1962.

[11] Y. Gault and H. Felkin, "Results of gas chromatography analysis," *Bull. Soc. Chim. France*, p. 742, 1965.

[12] D. J. Cram, F. A. A. Elhafez, and H. L. Nyquist, "Studies in Stereochemistry. XXI. Steric Control of Asymmetric Induction in the Preparation of the 2,5-Dimethyl-4-phenyl-3-hexanol System," *Journal of the American Chemical Society*, vol. 76, pp. 22–28, Jan. 1954.

[13] N. T. Anh and O. Eisenstein, "Induction asymetrique 1–2: comparaison ab initio des modeles de cram, de cornforth, de karabatsos et de felkin.," *Tetrahedron Letters*, vol. 17, no. 3, pp. 155–158, 1976.

[14] W. J. Hehre, W. A. Lathan, R. Ditchfield, M. D. Newton, and J. A. Pople, "Gaussian 70," 1970.

[15] H. Bürgi, J. Dunitz, J. Lehn, and G. Wipff, "Stereochemistry of reaction paths at carbonyl centres," *Tetrahedron*, vol. 30, pp. 1563–1572, Jan. 1974.

[16] C. E. Wintner, "Stereoelectronic effects, tau bonds, and Cram's rule," *J. Chem. Educ*, vol. 64, no. 7, p. 587, 1987.

[17] G. S. Hammond, "A Correlation of Reaction Rates," *Journal of the American Chemical Society*, vol. 77, pp. 334–338, Jan. 1955.

[18] Houk, "Theory and Modeling of Stereoselective Organic Reactions Author(s): Kendall N. Houk, Michael N. Paddon-Row, Nelson G. Rondan, Yun-Dong Wu, Frank K. Brown, David C. Spellmeyer, James T. Metz, Yi Li and Richard J. Loncharich," *Science, New Series*, vol. 231, no. 4742, pp. 1108–1117, 1986.

[19] G. Deslongchamps and P. Deslongchamps, "Bent bonds, the antiperiplanar hypothesis and the theory of resonance. A simple model to understand reactivity in organic chemistry," *Organic & Biomolecular Chemistry*, vol. 9, no. 15, p. 5321, 2011.

[20] G. Deslongchamps and P. Deslongchamps, "Bent bonds and the antiperiplanar hypothesis as a simple model to predict Diels–Alder reactivity: retrospective or perspective?," *Tetrahedron*, vol. 69, pp. 6022–6033, July 2013.

[21] G. Deslongchamps and P. Deslongchamps, "Bent bonds and the antiperiplanar hypothesis – a simple model to rationalize [1,3] -sigmatropic alkyl shifts," *Organic & Biomolecular Chemistry*, vol. 14, no. 32, pp. 7754–7767, 2016.

[22] G. Deslongchamps and P. Deslongchamps, "Bent Bonds (τ) and the Antiperiplanar Hypothesis—The Chemistry of Cyclooctatetraene and Other C_8 H_8 Isomers," *The Journal of Organic Chemistry*, vol. 83, pp. 5751–5755, May 2018.

[23] G. Deslongchamps and P. Deslongchamps, "Bent Bonds and the Antiperiplanar Hypothesis. A Model To Account for Sigmatropic [1, *n*]-Hydrogen Shifts," *The Journal of Organic Chemistry*, vol. 83, pp. 10383–10388, Sept. 2018.

[24] J. W. Cornforth, R. H. Cornforth, and K. K. Mathew, "24. A general stereoselective synthesis of olefins," *Journal of the Chemical Society (Resumed)*, pp. 112–127, 1959.

[25] E. J. Corey, "The Stereochemistry of α-Haloketones. I. The Molecular Configurations of Some Monocyclic α-Halocyclanones," vol. 75, p. 4, 1953.

[26] G. Wittig and U. Schöllkopf, "Triphenylphosphinemethylene as an olefin-forming reagent. I," *Chemische Berichte*, vol. 97, pp. 1318–30, 1954.

[27] E. J. Corey, "The Stereochemistry of α-Haloketones. VII. The Stereochemistry and Spectra of Some α-Chlorocyclohexanones," vol. 77, p. 3, 1955.

[28] D. A. Evans, S. J. Siska, and V. J. Cee, "Resurrecting the Cornforth Model for Carbonyl Addition: Studies on the Origin of 1,2-Asymmetric Induction in Enolate Additions to Heteroatom-Substituted Aldehydes," *Angewandte Chemie International Edition*, vol. 42, pp. 1761–1765, Apr. 2003.

[29] A. Mengel and O. Reiser, "Around and beyond Cram's Rule," *Chemical Reviews*, vol. 99, pp. 1191–1224, May 1999.

[30] M. Hayashi, T. Inoue, Y. Miyamoto, and N. Oguni, "Asymmetric carbon-carbon bond forming reactions catalyzed by chiral Schiff base-titanium alkoxide complexes," *Tetrahedron*, vol. 50, pp. 4385–4398, Apr. 1994.

[31] D. E. Ward, M. J. Hrapchak, and M. Sales, "Diastereoselective Formation of Cyanohydrins from α-Alkoxy Aldehydes," *Organic Letters*, vol. 2, pp. 57–60, Jan. 2000.

[32] A. Baeza, C. Nájera, J. M. Sansano, and J. M. Saá, "Binolam-AlCl: A Two-Centre Catalyst for the Synthesis of Enantioenriched Cyanohydrin O-Phosphates," *Chemistry - A European Journal*, vol. 11, pp. 3849–3862, June 2005.

[33] Molecular Operating Environment (MOE), 2013.08; Chemical Computing Group ULC, 1010 Sherbooke St. West, Suite #910, Montreal, QC, Canada, H3A 2R7, 2019.

[34] A. Lambropoulos and G. Deslongchamps, "GI-MOE," 2019.

[35] M. J. Frisch, G. W. Trucks, H. B. Schlegel, G. E. Scuseria, M. A. Robb, J. R. Cheeseman, G. Scalmani, V. Barone, B. Mennucci, G. A. Petersson, H. Nakatsuji, M. Caricato, X. Li, H. P. Hratchian, A. F. Izmaylov, J. Bloino, G. Zheng, J. L. Sonnenberg, M. Hada, M. Ehara, K. Toyota, R. Fukuda, J. Hasegawa, M. Ishida, T. Nakajima, Y. Honda, O. Kitao, H. Nakai, T. Vreven, J. J. A. Montgomery, J. E. Peralta, F. Ogliaro, M. Bearpark, J. J.

Heyd, E. Brothers, K. N. Kudin, V. N. Staroverov, T. Keith, R. Kobayashi, J. Normand, K. Raghavachari, A. Rendell, J. C. Burant, S. S. Iyengar, J. Tomasi, M. Cossi, N. Rega, J. M. Millam, M. Klene, J. E. Knox, J. B. Cross, V. Bakken, C. Adamo, J. Jaramillo, R. Gomperts, R. E. Stratmann, O. Yazyev, A. J. Austin, R. Cammi, C. Pomelli, J. W. Ochterski, R. L. Martin, K. Morokuma, V. G. Zakrzewski, G. A. Voth, P. Salvador, J. J. Dannenberg, S. Dapprich, A. D. Daniels, O. Farkas, J. B. Foresman, J. V. Ortiz, J. Cioslowski, and D. J. Fox, "Gaussian 09," 2010.

[36] MathWorks, "Matlab," 2015.

[37] Æ. Frisch, M. J. Frisch, F. R. Clemente, and G. W. Trucks, *Gaussian 09 User's Reference*. Gaussian Inc., 2nd ed., 2013.

[38] H. B. Burgi, J. D. Dunitz, and E. Shefter, "Geometrical reaction coordinates. II. Nucleophilic addition to a carbonyl group," *Journal of the American Chemical Society*, vol. 95, no. 15, pp. 5065–5067, 1973.

[39] H. B. Bürgi and J. D. Dunitz, "From Crystal Statics to Chemical Dynamics," *Accounts of chemical research*, vol. 16, no. 5, pp. 153–161, 1983.

[40] D. Y. Curtin, "Stereochemical control of organic reactions. Differences in behavior of diastereoisomers.," *Record Chem. Progr.*, vol. 15, pp. 111–28, 1954.

Appendix A

Postulates, Principles, and Angles

A.1 Hammond Postulate

The transition state is the most energetically expensive point of any reaction step, and for a multi-step reaction, the highest transition state is the rate-limiting step under kinetically controlled conditions. The Hammond Postulate allows one to infer transition state geometries depending on the reaction being exothermic or endothermic.[17] For exothermic reactions, the transition state is more energetically and geometrically similar to the reactants, suggesting minimal bond breaking/forming, and is associated with very reactive nucleophiles and electrophiles; it is referred to as an early transition state along the reaction coordinate. For endothermic reactions, the transition state is more energetically and geometrically similar to the products, suggesting more advanced bond breaking/forming, and is associated with less reactive nucleophiles and electrophiles; it is referred to as a late transition state. Closer proximity of the nucleophile to the electrophile at the transition state should bear more influence on the reaction outcome so later transition states should be more diastereoselective than earlier ones (Figure A.1).

A.2 Curtin-Hammett Principle

The Curtin-Hammett principle applies to situations where different products can be formed from potentially equilibrating substrates (or substrate conformers).[40] For the case of reversible reactions where two products can readily equilibrate, the product ratios are thermodynamically determined by the relative free energies of the two products. As shown in Figure A.2, product C would be formed preferentially over product D under thermodynamic conditions, regardless of the relative energies of reactant structures A and B. However, if the reactions are irreversible, by nature of the reactants or the specific reaction conditions, the outcome is kinetically controlled, and the product ratio would instead be determined by the relative activation energy barrier heights leading to products C and D. Thus the $\Delta\Delta G^{\ddagger}$ would determine the product ratio under kinetic conditions, regardless of the relative stabilities of reactant structures A and B. In the context of this study, the nucleophilic additions to carbonyl compounds (hydrides, Grignard reagents) are irreversible reactions and are under kinetic control. As a result, the Curtin-Hammett Principle states that the product ratios will depend on the relative activation energies ($\Delta\Delta G^{\ddagger}$) regardless

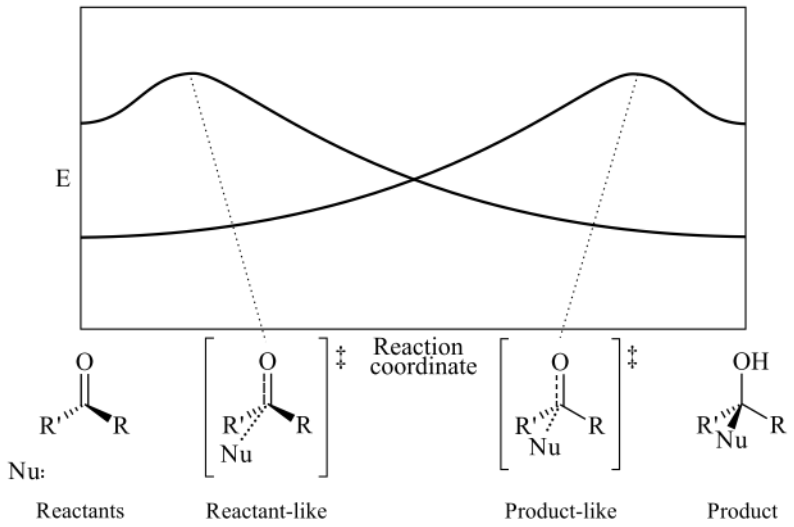

Figure A.1: Comparing the reaction profiles of an exothermic reaction (i.e. early transition state, reactant-like) and an endothermic reaction (i.e. late transition state, product-like). Chart reproduced from Hammond, 1955.[17]

of the relative product stabilities and, more importantly, regardless of the equilibrium ratio of reactant structures A and B. So diastereoselectivity models that are solely based on the relative stabilities of α-chiral carbonyl substrate conformers, or of any ground-state structures for that matter, contravene the Curtin-Hammett Principle and must be considered accordingly. For instance, older predictive models, such as the original Cram model, considered only ground-state reactant conformations. Ultimately, one must be mindful that a model is just that, a model, and may correctly predict the diastereoselectivity of a given reaction despite being derived from an inaccurate picture of the reaction parameters. Models that consider transition state structures for the predictive analysis are more consistent with our understanding of chemical reactivity and the Curtin Hammett Principle. This thesis studies diastereoselective reactions using quantum mechanically derived transition state structures, analyzing both their geometry and relative energies.

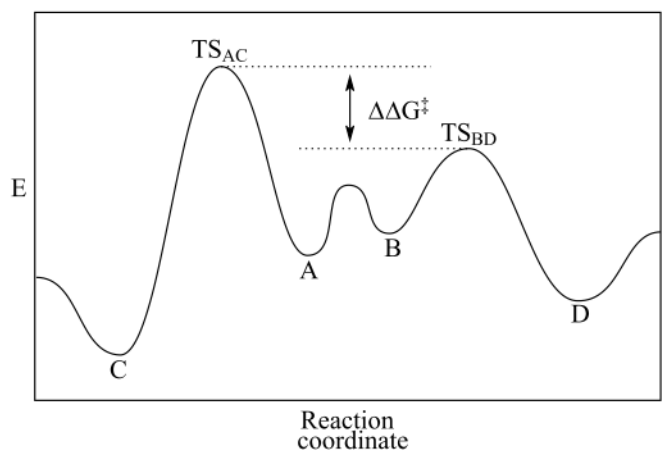

Figure A.2: Assuming a small difference in energy between A and B relative to transition states TSAC and TSBD, the ratio of the products C and D depends on $\Delta\Delta G^{\ddagger}$, the difference in activation energies between TSAC and TSBD.[40]

A.3 Bürgi-Dunitz Angle

H.-B. Bürgi and J. Dunitz reported the x-ray crystallographic structures of aminoketones that bear a carbonyl group and a nucleophilic nitrogen, all capable of interacting in intramolecular fashion.[39] The crystals revealed varying amounts of structural distortions, especially when the nitrogen was near the carbonyl group, that could be plotted for analysis. The frequency of data points on the plots gave an indication of the relative potential energies of the structures. In other words, high-energy distorted structures would occur less frequently than low-energy and less distorted counterparts. The geometries of the highest potential energy structures provided insight on the preferred trajectory of the intramolecular attack of the nucleophile to the carbonyl group. It was found that reactions of this type prefer a N····C=O angle of attack that is greater than 90°, and optimal at around 105° (Figure A.3). In this thesis, all the reactions involve intermolecular addition (i.e. bimolecular addition) so the N····C=O angle is likely to be somewhat wider than the 105° angle estimated from the conformationally restrained intramolecular systems of the Bürgi-Dunitz study.

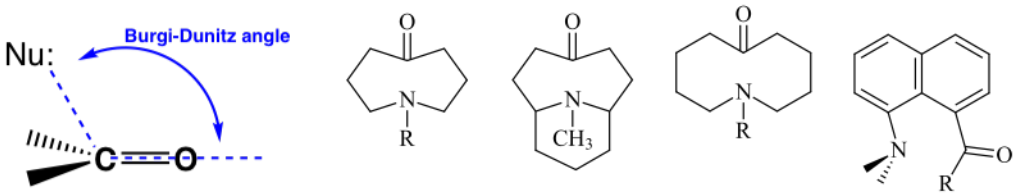

Figure A.3: Left: Bürgi-Dunitz angle. Right: Typical compounds investigated by X-ray crystallography. Reproduced from Bürgi, Dunitz 1983.[39]

Vita

Candidate's full name:	Jeffrey Douglas Retallick
Universities attended:	University of New Brunswick (2015)
	Bachelor of Science
	University of New Brunswick (2019)
	Masters of Science
Publications:	No publications
Conference Presentations:	No conferences attended